

CENTRAL RESEARCH LIBRARY
DOCUMENT COLLECTION

MARTIN MARIETTA ENERGY SYSTEMS LIBRARIES

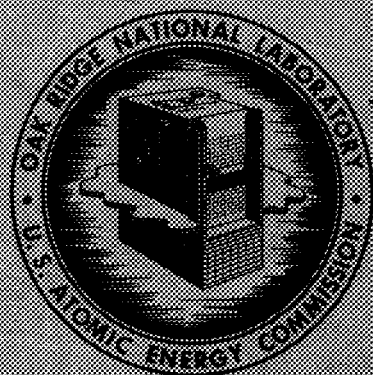


3 4456 0350331 3

ORNL-2195
Physics and Mathematics

A STUDY OF THE NUCLEAR AND
PHYSICAL PROPERTIES OF THE ORNL
GRAPHITE REACTOR SHIELD

T. V. Blosser	R. C. Reid
G. W. Bond	A. B. Reynolds
L. A. Lee	T. O. P. Speidel
D. T. Morgan	D. W. Vroom
J. F. Nichols	M. A. Welt



OAK RIDGE NATIONAL LABORATORY

operated by

UNION CARBIDE CORPORATION

for the

U.S. ATOMIC ENERGY COMMISSION

CENTRAL RESEARCH LIBRARY
DOCUMENT COLLECTION

LIBRARY LOAN COPY

DO NOT TRANSFER TO ANOTHER PERSON

If you wish someone else to see this document, send in name with document and the library will arrange a loan.

Printed in USA. Price 1.25 cents. Available from the
Office of Technical Services
U. S. Department of Commerce
Washington 25, D. C.

— LEGAL NOTICE —

This report was prepared as an account of Government sponsored work. Neither the United States, nor the Commission, nor any person acting on behalf of the Commission:

- A. Makes any warranty or representation, express or implied, with respect to the accuracy, completeness, or usefulness of the information contained in this report, or that the use of any information, apparatus, method, or process disclosed in this report may not infringe privately owned rights; or
- B. Assumes any liabilities with respect to the use of, or for damages resulting from the use of any information, apparatus, method, or process disclosed in this report.

As used in the above, "person acting on behalf of the Commission" includes any employee or contractor of the Commission to the extent that such employee or contractor prepares, handles or distributes, or provides access to, any information pursuant to his employment or contract with the Commission.

ORNL-2195 Erratum

Page iii

Lines 7 and 8 should read as follows:

.....
always placed behind the detectors to simulate a homogeneous shield.
The average relaxation length for gamma rays in barytes-haydite

Internal Distribution Only.

UNCLASSIFIED

ORNL-2195

Copy No. 5

Contract No. W-7405-eng-26

Neutron Physics Division

A STUDY OF THE NUCLEAR AND PHYSICAL PROPERTIES OF THE
ORNL GRAPHITE REACTOR SHIELD

T. V. Blosser	R. C. Reid*
G. W. Bond*	A. B. Reynolds*
L. A. Lee*	T. O. P. Speidel*
D. T. Morgan*	D. W. Vroom*
J. F. Nichols*	M. A. Welt*

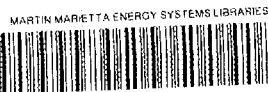
Date Issued

AUG 25 1958

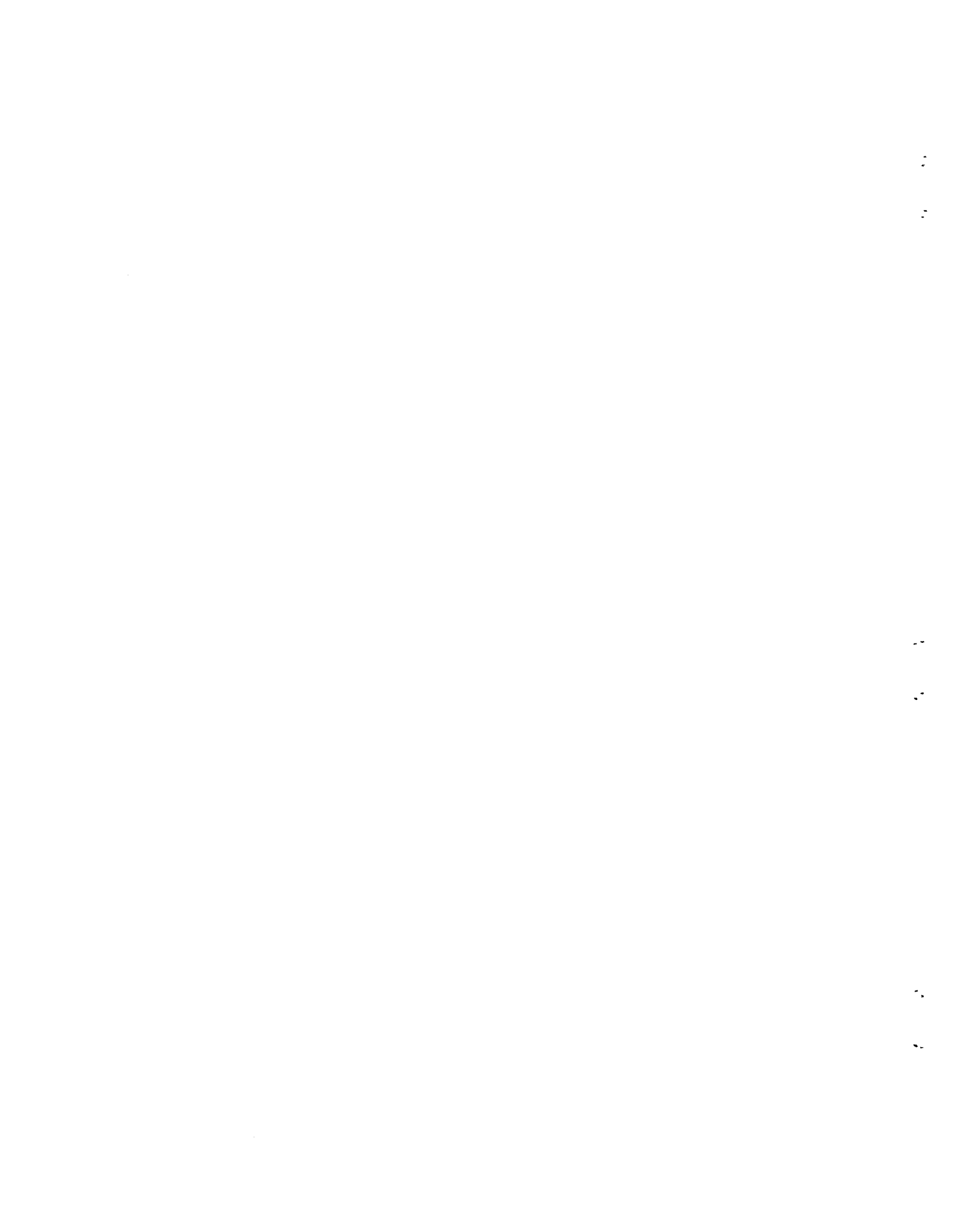
OAK RIDGE NATIONAL LABORATORY
Oak Ridge, Tennessee
operated by
UNION CARBIDE CORPORATION
for the
U. S. ATOMIC ENERGY COMMISSION

*MIT Engineering Practice School, Gaseous Diffusion Plant, Oak Ridge, Tennessee

UNCLASSIFIED



3 4456 0350331 3



ABSTRACT

A study of the nuclear and physical properties of the concrete shield of the ORNL Graphite Reactor was performed both to determine the radiation attenuation characteristics of the shield and to discover any effects of a long-term (12-year) irradiation. In the experiment neutron and gamma radiation measurements were made in a 4-5/8-in.-dia hole in the shield as the hole was drilled in increments of 1 or 1/2 ft. Concrete plugs were always placed behind the detectors to simulate a homogeneous shield. Average relaxation lengths for gamma rays ~~and fast neutrons~~ in barytes-haydite concrete, of which most of the shield is made, is approximately 13.6 cm, increasing gradually from 13.0 cm at a shield thickness of 2 ft to 14.6 cm at a shield thickness of 5 ft. The fast-neutron relaxation length in the barytes-haydite concrete varied from 10.0 cm to 10.6 cm, the average being approximately 10.2 cm. Measurements of the streaming of radiation through the hole were also made. The concrete dust collected from the drillings was used to determine the chemical composition, water content, density, compressive strength, and radioactivity of the shield at the various depths. The temperature gradient through the shield was also measured. This investigation showed that the chemical properties and density of the shield have not changed appreciably since a similar investigation in 1948, but its compressive strength is lower ($\sim 40\%$ near the reflector-shield interface).

TABLE OF CONTENTS

	<u>Page No.</u>
Abstract	iii
Introduction	1
I. Description of the Shield	2
II. Experimental Procedure	3
III. Physical and Chemical Properties of the Shield	5
Chemical Composition	5
Water Content	7
Density	10
Compressive Strength	10
Concrete Activity	11
Temperature Gradient Through Shield	13
IV. Radiation Attenuation Measurements in the Shield	15
Gamma-Ray Dose Rates	15
Personnel Monitoring Film Measurements	20
Ionization Chamber Measurements	21
Fast-Neutron Dose Rates	23
Thermal-Neutron Flux Measurements	29
Foil Measurements	29
Calculation of the Flux from the Foil Measurements	32
App. A. List of Tables	37
App. B. List of Figures	38

INTRODUCTION

The numerous factors involved in reactor shield design require that both experimental and theoretical values of neutron and gamma-ray attenuations be known in order to design an economical radiation-safe shield. One of the cheapest and most commonly used materials for shielding around stationary reactors is concrete, and the oldest existing concrete shield is the shield around the ORNL Graphite Reactor. This shield consists of a 5-ft thickness of barytes-haydite concrete sandwiched between two 1-ft thicknesses of ordinary Portland concrete. In order to obtain experimental data from which the shielding properties of the concrete could be determined and at the same time to discover any changes in the structural properties of the concrete which had served as a shield for several years, a study of the nuclear and physical properties of the concrete around the ORNL Graphite Reactor was undertaken. The shielding portion of the study included measurements of the gamma-ray, fast-neutron, and thermal-neutron intensities in a 4-5/8-in.-dia hole as the hole was drilled through the shield. The physical and chemical properties of the shield were determined from the concrete removed by the core-type drill. At the time this investigation was performed (February - July 1956) the shield had been in place for 12 years.

An investigation similar to the one reported here was conducted previously at the ORNL Graphite Reactor,^{1,2} but it yielded results of limited usefulness since water was introduced into the hole both to cool and clean the drill bit and to provide personnel shielding. The effect of the water on the measurements could not be determined. Similar studies were also carried out at the BEPO at Harwell, England,³ at the Brookhaven Reactor at Brookhaven National Laboratory,⁴ and at the JEEP at Kjeller, Norway,⁵ but in every case

1. T. Rockwell, III, "Physical Tests on Core Drillings from the ORNL Graphite Reactor Shield," ORNL-241 (1949).
2. S. W. W. Shor and J. M. Cassidy, "Effect of Water Soaking on Shielding Properties of the Oak Ridge Pile Shield," ORNL-203 (1949).
3. J. R. Harrison, A. M. Mills, and D. Bedell, "The Distribution of Gamma-Rays and Neutrons in the Control Face of the BEPO," AERE RP/R-1604 SWP/P20 (1955).
4. W. W. Pratt, et al., "The Attenuation Characteristics of Brookhaven Concrete," BNL-145 (1951).
5. F. Adler and H. Klepp, "Thermal Neutron Distribution in the Concrete Shield of JEEP," Nucleonics 13, No. 2, 72 (1955).

there were adverse effects that prevented accurate interpretation of the results. The usefulness of the attenuation measurements made on the BEPO shield is limited by the absence of a chemical analysis of the concrete, especially of the water content. In the Brookhaven experiment a hole in the shield was plugged with blocks of concrete to simulate the shield thicknesses, and all measurements were made at the face of the shield using a collimator. The effects of radiation streaming around the plugs and of the geometry of the collimator could not be separated from other effects. In the experiment at the JEEP reactor at Kjeller the thermal-neutron flux throughout the shield was determined by irradiating foils embedded in two long concrete plugs placed in an existing hole. Again the streaming around the plugs had an adverse effect on the results.

In the experiment reported on the following pages radiation intensities were measured at the "bottom" of the hole immediately following the removal of a core drilling, a procedure which eliminated any streaming around plugs. In addition, each detector was positioned in a hollowed end of a concrete

plug, which gave the effect of embedding the detector in a homogeneous shield. In order to avoid introducing water into the hole the drill bit was cooled with air. By taking these precautionary measures the resulting data is unbiased by undeterminable effects.

I. DESCRIPTION OF THE SHIELD

The three sections of the 7-ft-thick ORNL Graphite Reactor shield are shown in Fig. 1. A 2.3-cm-thick layer of asbestos separates the concrete from the graphite lattice. The inner foot of the shield, adjacent to the graphite lattice, and the outer foot of the shield both consist of ordinary Portland concrete. Sandwiched between these two 1-ft

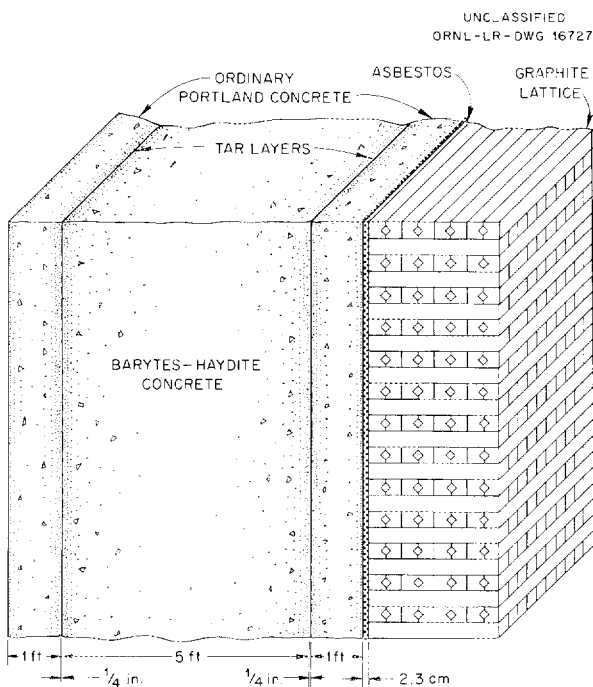


Fig. 1. Cross Section of ORNL Graphite Reactor Shield.

sections is a 5-ft thickness of barytes-haydite concrete covered with a bituminous coating (~ 0.5 cm thick) to prevent water evaporation. The barytes (BaSO_4) aggregate was added to the concrete to increase its density and the haydite, which is calcined shale, was added to increase the water content.

For this experiment it was arbitrarily decided to specify the shield thickness as the distance measured from the face of the graphite lattice. Therefore, each shield thickness reported here includes, in addition to the concrete, the layer of asbestos and the water-proofing tar coatings. It also includes the distance from the front of the instrument being used to its center of detection.

II. EXPERIMENTAL PROCEDURE

The 4-5/8-in.-dia experimental hole was drilled through the shield in increments of 1 or 1/2 ft at the center of the south face of the reactor. Gamma-ray and fast-neutron dose rates and thermal-neutron fluxes were measured after each incremental drilling,* rather than behind plugs in the hole, so that radiation leakage down a plug annulus would be avoided. A homogeneous concrete shield around each detector was simulated by placing the detector in a recession in one end of a close-fitting 14-in.-long concrete plug. This plug was made of the same type of concrete as that in the shield at the particular depth at which measurements were being made. Behind this 14-in.-long plug was placed a 5-ft-long plug of barytes-haydite concrete when the hole was deep enough to require it.

The hole through the outside 4 ft of shield was drilled in four 1-ft increments. The inner 3 ft of the hole was drilled in 1/2-ft increments, giving a total of 10 drillings. Each drilling was made during the normal weekly reactor shutdown and all attenuation measurements were made during the remainder of the week. In tabulating the results in this report, data listed under a given drilling number were taken during the week following that

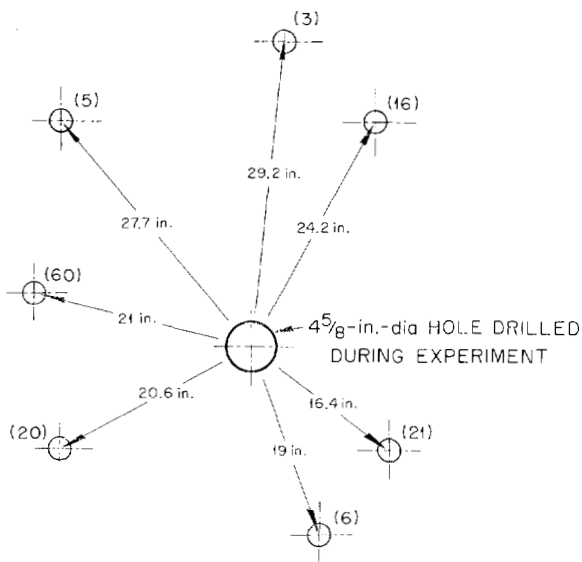
*Fast-neutron fluxes were also measured by activation of threshold foils, but there is considerable uncertainty in the results. These measurements are reported under separate cover in ORNL-CF-58-8-1, "Fast-Neutron Flux Measurements in the ORNL Graphite Reactor Shield," by T. V. Blosser et al. (1958).

particular drilling. For example, at Drilling 1 the first foot of the hole was drilled so attenuation data listed under this drilling were taken at a shield thickness of ~ 6 ft. Drilling 0 refers to data taken at the outside face of the shield. Attenuation measurements were made after Drilling 3 both before and after some graphite plugs in the neighboring experimental holes were replaced with concrete plugs and the results are listed under Drillings 3A and 3B, respectively.

The hole for the experiment was drilled as near the center of the south face as possible under the condition that it be approximately equidistant

UNCLASSIFIED
2-01-058-0-376

from neighboring experimental holes. The relative positions of these holes to the hole drilled in this experiment are shown in Fig. 2.



NOTE: NUMBERS IN PARENTHESES REFER TO EXPERIMENTAL HOLE NOS.

Fig. 2. Relative Location of $4\frac{5}{8}$ -in.-dia Hole with Respect to Adjacent Experimental Holes on South Face of ORNL Graphite Reactor.

Drilling a foot through the ordinary concrete required approximately 1 hr, while drilling through a foot of barytes-haydite concrete required only 15 min. A total of four diamond bits were dulled during the entire 7 ft of drilling.

The hole was drilled with a $4\frac{5}{8}$ -in.-dia diamond-edged core-type drill powered by a four-cylinder gasoline Hercules engine and forced into the shield by hydraulic pressure. Compressed air rather than water was used to cool the drill in order to avoid the introduction of water into the shield. The compressed air proved to be a sufficient coolant although frequent stops to allow the bit to cool were necessary when the ordinary Portland concrete was being drilled. No stops were necessary when drilling through the softer barytes-haydite concrete.

Radioactive dust which was produced during the drilling was collected in a vacuum cleaner system composed of four filter bags in a vacuum-tight box followed by a Pullman commercial type 1-1/4-hp vacuum cleaner. The dust collected in a removable filter in the vacuum cleaner provided representative concrete samples for chemical analysis. A new filter was used for each drilling.

After each drilling was completed, the concrete core was broken from the shield by a wedge driven between the drill and the core. Fortunately, the end of the core consistently broke off evenly so that the uncertainty in the depth of the hole was less than a centimeter. The core was removed and sealed in a polyethylene bag, and the depth of the hole from the outer surface was then measured. Following the final drilling the depth to the graphite lattice was measured; all hole depths could then be converted to shield thicknesses.

The core removed from the outside foot of the shield (ordinary concrete) is shown in Fig. 3. The steel reinforcement rods shown crossing the core were the only rods encountered during the entire drilling of the hole.

In order to avoid confusion as to which end of the drilled hole is being referred to, the term "bottom" of the hole is used throughout this report in referring to the end of the hole inside the shield, i.e., nearest the graphite lattice, even though the hole was drilled horizontally.

III. PHYSICAL AND CHEMICAL PROPERTIES OF THE SHIELD

After each drilling, except drillings 3, 4, and 7, the chemical composition of the concrete was determined by both chemical and spectrographic analyses. A spectrographic analysis of an asbestos sample was also made. In addition, the following physical properties of the concrete cores removed from the hole were determined: water content, density, compressive strength, and radioactivity. The temperature gradient throughout the shield was also determined.

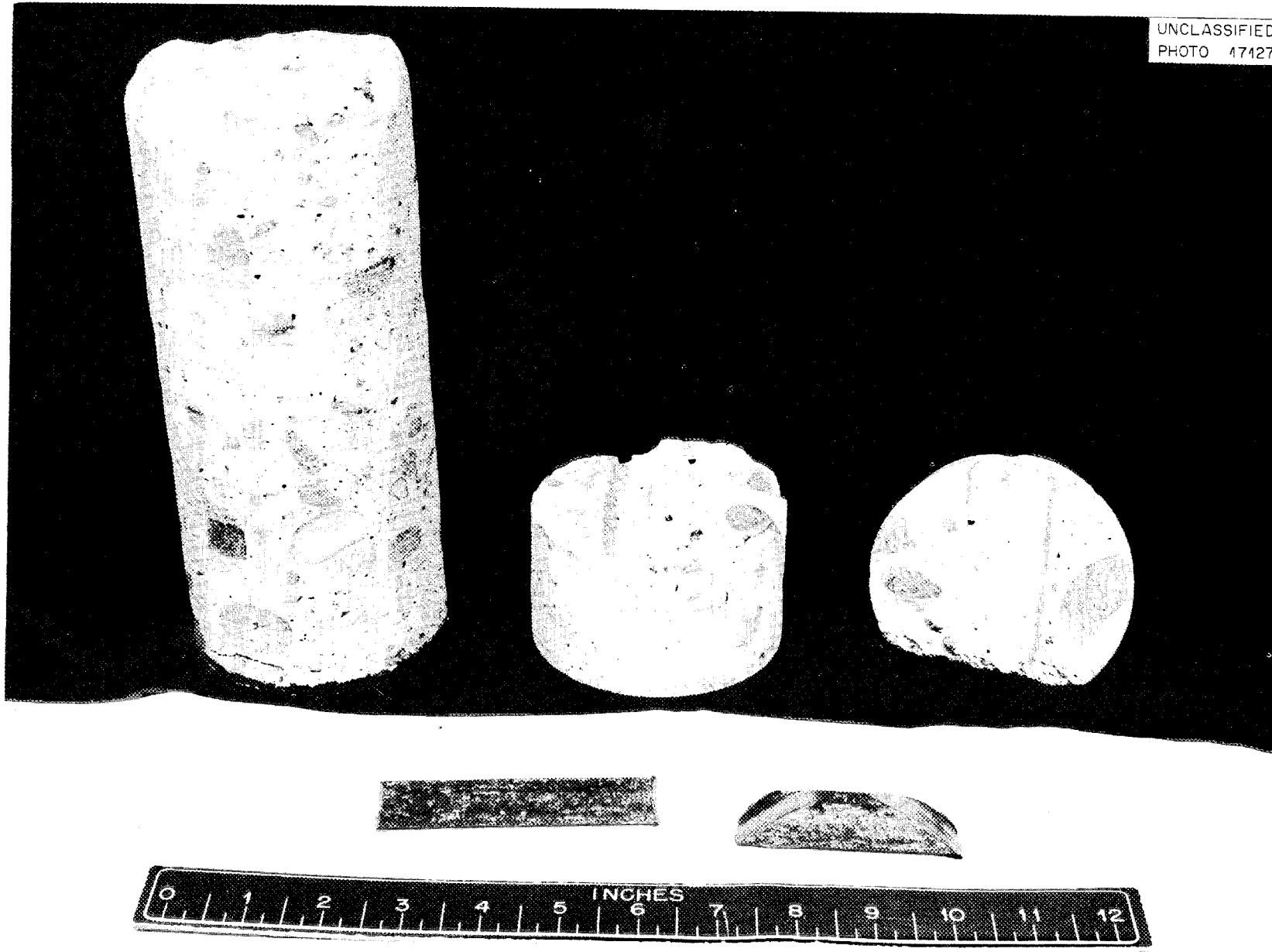
Chemical Composition

Since the chemical and spectrographic analyses were made from concrete dust which was collected in the vacuum-cleaner filter during each drilling, a representative sample of the concrete for that portion of the shield was obtained. All analyses were made by the Analytical Chemistry Division of ORNL.

When poured, the composition of the concrete in this section was:¹

Cement (Portland, low heat)	16.3 wt%	Barytes aggregate	46.4 wt%
Haydite	27.3 wt%	Water	10.0 wt%

UNCLASSIFIED
PHOTO 47127



9
-

Fig. 3. Core Drilled from Outside Foot of ORNL Graphite Reactor Shield. This portion of the shield was ordinary Portland cement concrete. Steel rods in foreground are reinforcement rods encountered in the first foot of drilling.

The composition of the haydite, a porous calcined shale, was assumed to be:

SiO ₂	60 wt%	Al	8.5 wt%
Al ₂ O ₃	16 wt%	Ca	17.0 wt%
CaO	24 wt%	Si	48 wt%

The barytes aggregate was 96.4% BaSO₄. The BaSO₄ consisted of equal parts of aggregates as follows:

<u>A</u>	<u>B</u>
100% through 7/8-in. screen	100% through 4-mesh screen
5.25% through 8-mesh screen	0-5% through 100-mesh screen
Fineness modulus = 5.95 - 5.20	Fineness modulus = 3.33 - 2.58

The results of the chemical analyses for each drilling are presented in Table 1. These analyses were performed on a dry basis. Oxygen not present as water could not be determined analytically but can be approximated by difference.

Results of the spectrographic analyses of the concrete samples are given in Table 2, along with a spectrographic analysis of asbestos separating the graphite lattice from the concrete shield. The original chemical analysis of the asbestos was unavailable.

Water Content

The results of the water content analyses, also determined by the Analytical Chemistry Division of ORNL, are presented in Table 3. Duplicate samples were analyzed for Drilling 10.

Table 3. Water Content, Density, and Compressive Strength of Samples of Concrete from the ORNL Graphite Reactor Shield

Drilling No. ^a	Shield Thickness (ft)	Water Content (wt%), This Study	Density (g/cc)		Compressive Strength (psi)	
			This Study	1948 ^b	This Study	1948 ^b
1	6 - 7	6.73	2.22	2.20	1605	1650
2	5 - 6	9.96	2.26	2.27	2410	2460
3	4 - 5	11.9	2.35	2.28	2550	2775
4	3 - 4	12.0	2.34	2.26	2320	2891
5	2.5 - 3	10.2	2.36	2.17	3970	2980
6	2 - 2.5	13.2	2.34	2.17	2140	2953
7	1.5 - 2	15.0	2.35	2.16	2050	2765
8	1 - 1.5	13.5	2.15	1.96	1585	2170
9	0.6 - 1	9.24	2.36	2.21	1610	2676
10	0 - 0.6	6.93	2.54	2.11	1470	2450

a. Drillings 1, 9, and 10 were in Portland concrete; other drillings were in barytes-haydite concrete.

b. Average values from Ref. 1.

Table 1. Chemical Analysis (Dry Basis) of Samples of Concrete
from the ORNL Graphite Reactor Shield^a

Element	Composition (wt%)						
	Drilling 1, 6 - 7 ft of Shield	Drilling 2, 5 - 6 ft of Shield	Drilling 5, 2.3 - 3 ft of Shield	Drilling 6, 2 - 2.5 ft of Shield	Drilling 8, 1 - 1.5 ft of Shield	Drilling 9, 0.6 - 1 ft of Shield	Drilling 10, 0 - 0.6 ft of Shield
Fe	1.58	1.14	1.23	2.20	1.36	1.27	1.24
Mg	2.37	2.41	1.97	0.004	0.35	0.50	0.35
Ca	11.31	11.00	8.00	9.69	8.0	7.75	6.88
Si	33.65	10.24	9.96	10.54	10.07	35.01	33.59
S	0.66	0.66	0.27	0.28	0.44	0.31	0.47
Al	1.57	2.09	2.47	2.22	3.19	2.58	2.73
Na	0.20	-	-	-	0.17	0.14	0.12
K	0.30	-	-	-	0.40	0.11	0.14
Ba	-	27.00	27.90	18.20	28.60	-	-
C	-	-	-	3.88	0.71	0.82	0.73
H	b	b	b	b	b	b	b
O	c	c	c	c	c	c	c

- a. Drillings 1, 9, and 10 were in Portland concrete; other drillings were in barytes-haydite concrete.
b. Too low for analysis.
c. Not attainable.

Table 2. Spectrographic Analysis of Samples of Concrete from ORNL Graphite Reactor Shield^a

Element	Limit of Detection (%)	Composition ^b (wt%)							Asbestos
		Drilling 1, 6 - 7 ft Of Shield	Drilling 2, 5 - 6 ft Of Shield	Drilling 5, 2.5 - 3 ft Of Shield	Drilling 6, 2 - 2.5 ft Of Shield	Drilling 8, 1 - 1.5 ft Of Shield	Drilling 9, 0.6 - 1 ft Of Shield	Drilling 10, 0 - 0.6 ft Of Shield	
Ag	0.0001	-	-	-	-	-	-	-	-
Al		B	B	B	C-D	C	B	B	D
As	0.3	-	-	-	-	-	-	-	-
Au	0.004	-	-	-	-	-	-	-	-
B	0.008	D	E	E	-	E	-	-	-
Ba	0.02	-	-	B	A-B	B	-	-	-
Be	0.0005	-	-	-	-	-	-	-	-
Bi	0.001	-	-	-	-	-	-	-	-
Ca		A	A	A	A	-	A	A	E
Cd	0.022	-	-	-	-	-	-	-	-
Co	0.002	-	-	-	-	-	-	-	-
Cr	0.0005	E	-	-	-	E	E	E	E
Cu		E	F	F	F	F	F	F	F
Fe		C	B	C	B	C	C	C	C
Ga	0.003	-	-	-	-	-	-	-	-
Hg	0.06	-	-	-	-	-	-	-	-
K	1.4	-	-	-	-	-	-	-	-
Li	0.054	-	-	-	-	-	-	-	-
Mg		B	B	C	-	B	B	B	A
Mn		C	C	D	C	D	D	D	D
Mo	0.001	-	-	-	-	E	-	-	-
Na	0.04	C	C	-	-	D	E	D	-
Ni	0.002	-	E	-	-	E	-	F	E
Pb	0.01	-	-	-	-	D	-	-	-
Pd	0.0009	-	-	-	-	-	-	-	-
Pt	0.009	-	-	-	-	-	-	-	-
Ru	0.005	-	-	-	-	-	-	-	-
S		C	-	-	-	-	-	-	-
Sb	0.014	-	-	-	-	-	-	-	-
Si		A	A	A	B	B	B	B	B
Sn	0.003	-	-	-	-	E	-	-	-
Sr		-	-	-	-	C	E	E	-
Ta	0.1	-	-	-	-	-	-	-	-
Ti		D	C	D	C-D	D	D	D	-
Tl	0.05	-	-	-	-	-	-	-	-
V	0.004	-	-	-	-	E	-	-	-
W	0.09	-	-	-	-	-	-	-	-
Zn	0.12	-	-	-	-	-	-	-	-
Zr	0.008	-	D	-	-	-	E	E	-

a. Drillings 1, 9, and 10 were in Portland concrete; other drillings were in barytes-haydite concrete.

b. Legend: A, 10 to 100 wt%; B, 1 to 10 wt%; C, 0.1 to 1 wt%; D, 0.01 to 0.1 wt%; E, 0.001 to 0.01 wt%; F, 0.0001 to 0.001 wt% when a dash (-) appears it indicates that an analysis was made for the element but none was found. When no mark appears no analysis was made.

At the completion of each drilling the concrete core removed was immediately sealed in a polyethylene bag to insure that no change in moisture content occurred. After sufficient time had been allowed for decay of the radioactivity, a small portion of the core was sawed off and crushed. The sum of the combined and uncombined water was then determined by weighing the sample before and after heating it to 520°C. Several samples which were heated to 900°C showed little or no further change in weight.

Density

The density of the concrete was determined by weighing a portion of the core removed during the drilling and then determining its volume by water displacement. The results of the present investigation, together with the results from similar measurements made in the 1948 experiment¹ are also presented in Table 3. The concrete from the 1948 drilling came from the west face of the reactor.

Compressive Strength

Results of the compression tests on the concrete cores, together with the results reported in the 1948 investigation,¹ are also included in Table 3. The cores were tested according to ASTM standards (ASTM C42-49). A 30,000-lb testing machine located at the ORNL Graphite Reactor building was used to test the Portland concrete samples (Drillings 1, 9, and 10) and the last barytes-haydite sample (Drilling 8). The barytes-haydite core from Drilling 2 could not be broken on the 30,000-lb machine. When it was tested on a hydraulic ram, it was shattered by a dynamic force lower than the static loading (2410 psi) it had previously withstood in the 30,000-lb machine. All other barytes-haydite cores were tested on a 120,000-lb machine by E. R. Taylor of the Metallurgy Division at the Gaseous Diffusion Plant. The reason for the unusually large result for Drilling 5 could not be determined.

Concrete Activity

The concrete samples for activity measurements each weighed approximately 1 g and were prepared from the concrete dust removed during each drilling. Since it was not possible to measure the activity immediately after the drilling was completed, the sample of dust was later weighed and irradiated again in the hole in its original location for two to three days. Thus the short half-lived components of the concrete were saturated when the sample was again removed from the hole just prior to counting. The results are given in Table 4 and plotted in Fig. 4 as a function of the decay time for various shield thicknesses. Activities for this thicknesses greater than 4 ft were too low to count.

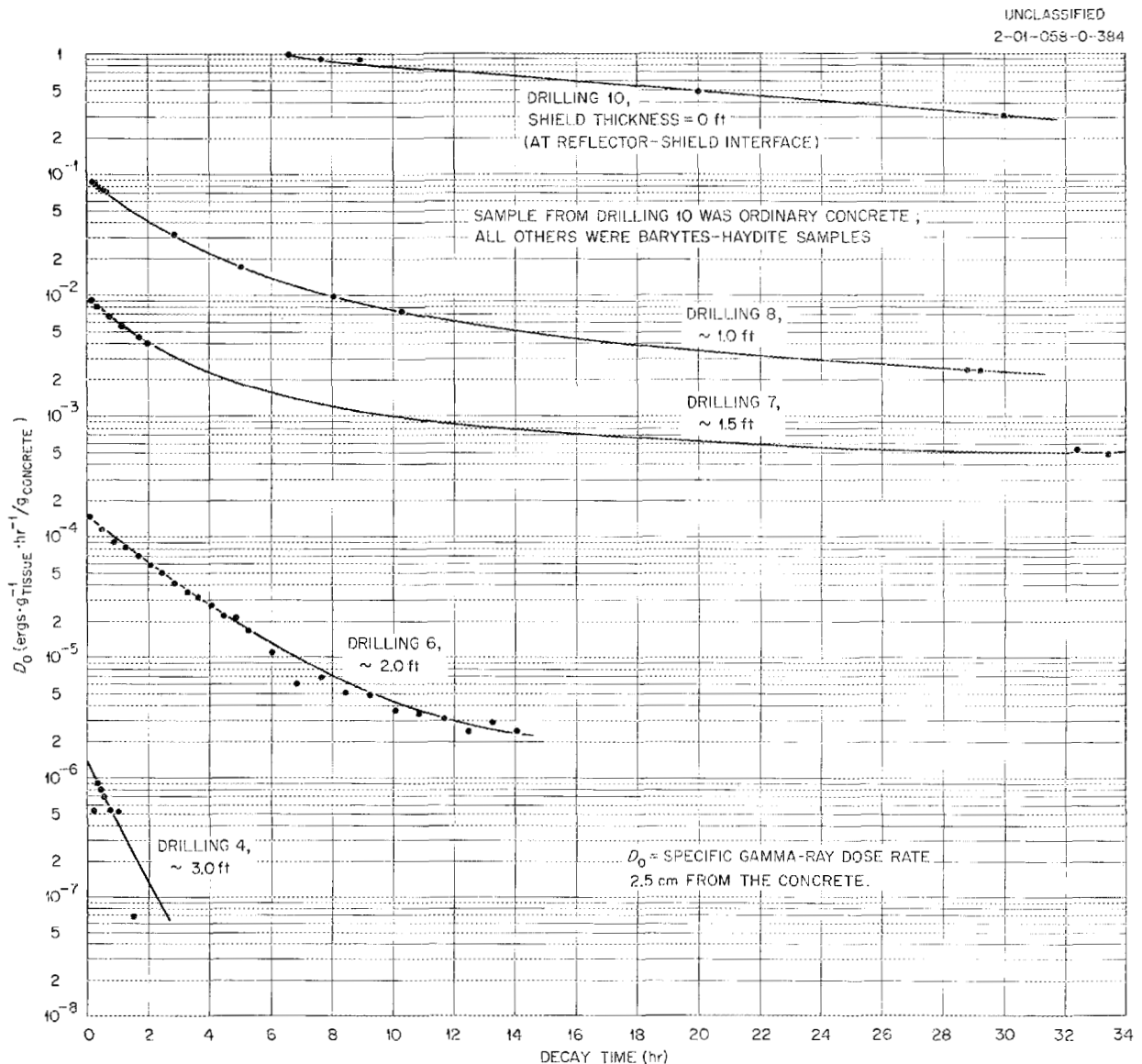


Fig. 4. Decay of Activity in the Concrete Samples Removed from the ORNL Graphite Reactor Shield After Each Core Drilling.

Table 4. Decay of Gamma-Ray Activity in Samples of Concrete from the ORNL Graphite Reactor Shield^a

Decay Time (hr)	Dose Rate ^b ($\frac{\text{ergs/g}_{\text{tissue}} \cdot \text{hr}}{\text{g}_{\text{concrete}}}$)	Decay Time (hr)	Dose Rate ^b ($\frac{\text{ergs/g}_{\text{tissue}} \cdot \text{hr}}{\text{g}_{\text{concrete}}}$)
Drilling 10, No Shield			
6.66	9.6×10^{-1}	30.0	2.91×10^{-1}
7.73	8.92×10^{-1}	50.0	1.2×10^{-1}
9.00	8.34×10^{-1}	60.0	7.66×10^{-2}
20.0	4.66×10^{-1}		
Drilling 8, ~1 ft of Shield			
0.20	8.68×10^{-2}	2.88	3.16×10^{-2}
0.30	8.25×10^{-2}	5.08	1.69×10^{-2}
0.38	7.92×10^{-2}	8.08	9.47×10^{-3}
0.48	7.60×10^{-2}	10.36	7.08×10^{-3}
0.55	7.49×10^{-2}	28.86	2.24×10^{-3}
0.65	7.07×10^{-2}	29.36	2.19×10^{-3}
Drilling 7, ~1.5 ft of Shield			
0.15	9.00×10^{-3}	1.69	4.46×10^{-3}
0.35	8.07×10^{-3}	1.99	3.98×10^{-3}
0.75	6.66×10^{-3}	32.53	4.94×10^{-4}
1.16	5.49×10^{-3}	33.53	4.49×10^{-4}
Drilling 6, ~2.0 ft of Shield			
0.069	1.47×10^{-4}	5.269	1.67×10^{-5}
0.468	1.15×10^{-4}	6.069	1.09×10^{-5}
0.869	9.09×10^{-5}	6.869	5.88×10^{-6}
1.269	8.18×10^{-5}	7.669	6.76×10^{-6}
1.669	6.84×10^{-5}	8.469	5.10×10^{-6}
2.069	5.80×10^{-5}	9.269	4.83×10^{-6}
2.469	4.97×10^{-5}	10.069	3.58×10^{-6}
2.869	4.11×10^{-5}	10.869	3.33×10^{-6}
3.269	3.46×10^{-5}	11.669	2.98×10^{-6}
3.669	3.17×10^{-5}	12.469	2.35×10^{-6}
4.069	2.70×10^{-5}	13.269	2.76×10^{-6}
4.469	2.22×10^{-5}	14.069	2.35×10^{-6}
4.869	2.12×10^{-5}		
Drilling 4, ~3.0 ft of Shield			
0.216	5.40×10^{-7}	0.762	5.38×10^{-7}
0.349	8.97×10^{-7}	1.032	5.19×10^{-7}
0.449	8.00×10^{-7}	1.495	6.90×10^{-8}
0.582	6.88×10^{-7}		

a. Drillings 1, 9, and 10 were in Portland concrete; other drillings were in barytes-haydite concrete.

b. Specific gamma-ray dose rate 2.5 cm from concrete.

Temperature Gradient Through Shield

Heating of the shield resulted both from heat leakage from the reactor core to the shield and from heat generation in the concrete itself caused by the transmission of radiation in the shield. The temperature gradient in the shield was assumed to be at a steady state after the reactor had been operating at full power (3500 kw) for five days. It was then measured by 12 iron-constantan thermocouples embedded along the central axis of a close-fitting, 7-ft-long concrete plug constructed to match the adjacent concrete of the shield. Since the reactor is air cooled and the inlet air temperature varies, thermocouples 1 and 12 were placed on the ends of the concrete plug to measure the ambient temperature of the inner and outer surface of the concrete shield. The small annular air gap surrounding the plug was stagnant and therefore did not appreciably affect the results, which are given in Fig. 5 and Table 5.

Table 5. Temperature Gradient Throughout the ORNL Graphite Reactor Shield

Shield Thickness		Temperature ($^{\circ}\text{C}$)		
(ft)	(cm)	During 3500-kw Operation ^a	5 hr After Shutdown ^a	10 hr After Shutdown ^b
0	0	40.0	32.1	29.2
0.083	2.5	37.5	33.4	30.5
0.125	3.8	36.0	33.4	31.0
0.542	16.5	34.7	33.9	31.2
0.958	29.2	32.8	32.6	30.5
1.4	41.9	31.2	30.6	29.9
2.04	62.2	27.5	27.8	27.7
3.04	92.7	24.0	24.5	24.8
4.04	123	22.0	22.1	22.4
5.29	161	20.3	20.2	20.2
6.54	199	19.9	19.9	20.1
7.00	213	19.0	19.0	20.0

a. Room temperature = 19°C .

b. Room temperature = 20°C .

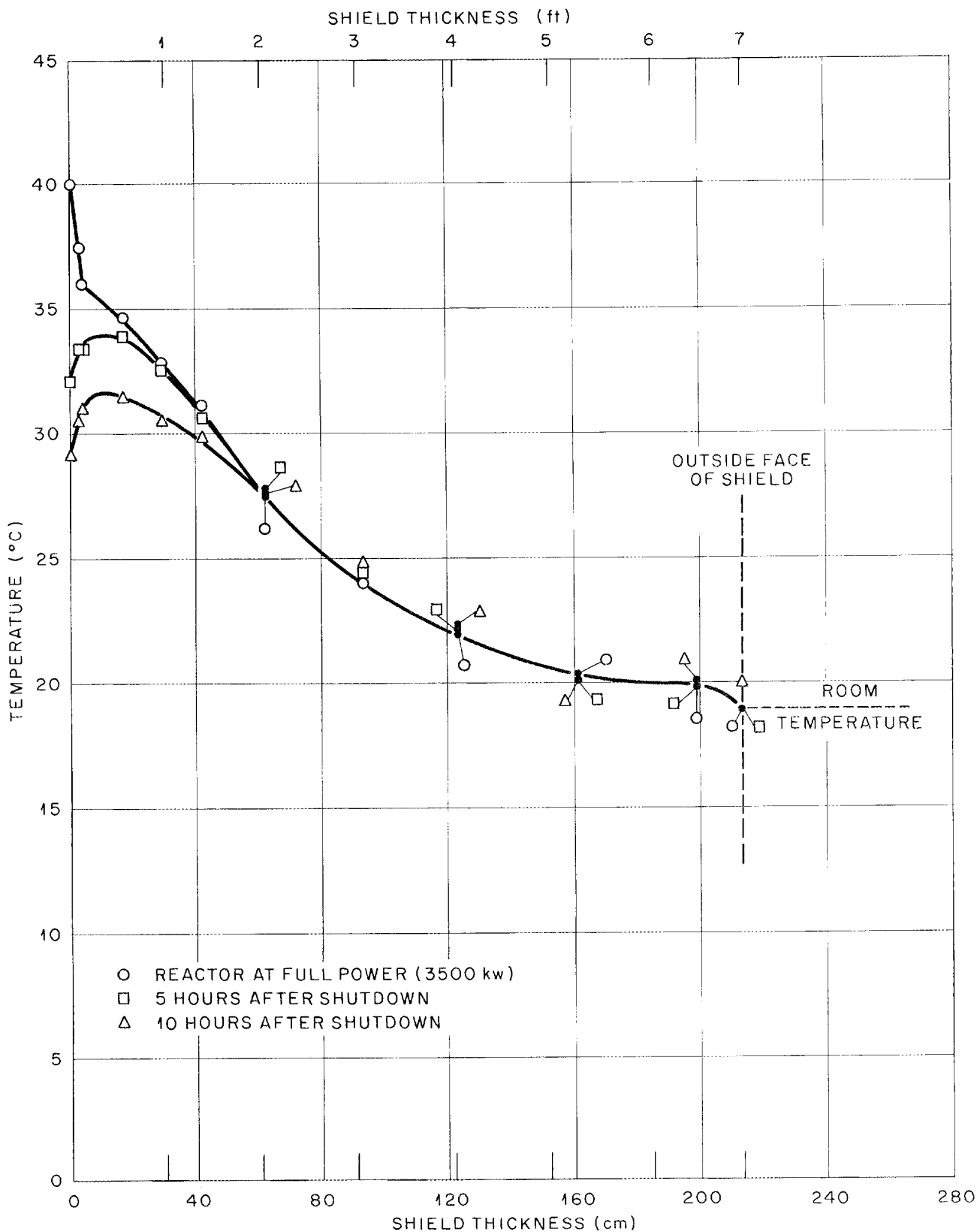


Fig. 5. Temperature Gradient Throughout ORNL Graphite Reactor Shield During 3500-kw Operation and 5 and 10 hr After Shutdown.

When the reactor is shut down, the air flow through the reactor is reduced by 60 to 70%. In order to determine the effect of this reduction on the shield temperature, the temperature gradient of the shield was again measured 5 and 10 hr after shutdown. The results of these measurements are also shown in Fig. 5 and Table 5.

IV. RADIATION ATTENUATION MEASUREMENTS IN THE SHIELD

The gamma-ray dose rates, fast-neutron dose rates, and thermal-neutron fluxes are all plotted together on Fig. 6 and measured as a function of the thickness of the ORNL Graphite Reactor Shield. The gamma-ray dose rates and fast-neutron dose rates are both given in ergs per gram of tissue per hour, and the thermal-neutron fluxes are presented as neutrons per square centimeter per second. As mentioned previously, the shield thicknesses indicated include the 2.3-cm thickness of asbestos covering the graphite reflector and the two ~ 0.5 -cm-thick layers of tar separating the Portland concrete from the barytes-haydite concrete. In some cases the shield thickness also includes the distance from the front face of an instrument to its center of detection as discussed below.

Average relaxation lengths for gamma rays and fast neutrons in barytes-haydite concrete were estimated from the attenuation curves in Fig. 6. The average gamma-ray relaxation length is approximately 13.6 cm. It can be seen from Fig. 6 that the gamma-ray relaxation length gradually increases with increasing shield thickness from 13.0 cm at a shield thickness of 2 ft to 14.6 cm at a shield thickness of 5 ft. The fast-neutron relaxation length in the barytes-haydite concrete is more constant, varying from 10.0 cm to 10.6 cm across the barytes-haydite section of the shield. The average fast-neutron relaxation length is approximately 10.2 cm.

Gamma-Ray Dose Rates

The gamma-ray dose rates were measured as a function of shield thickness by the use of a 50-cc carbon-wall ionization chamber and gamma-ray sensitive film packets. The results of both methods are presented in Table 6 and Fig. 7. The dose rates resulting from gamma rays streaming down the hole were

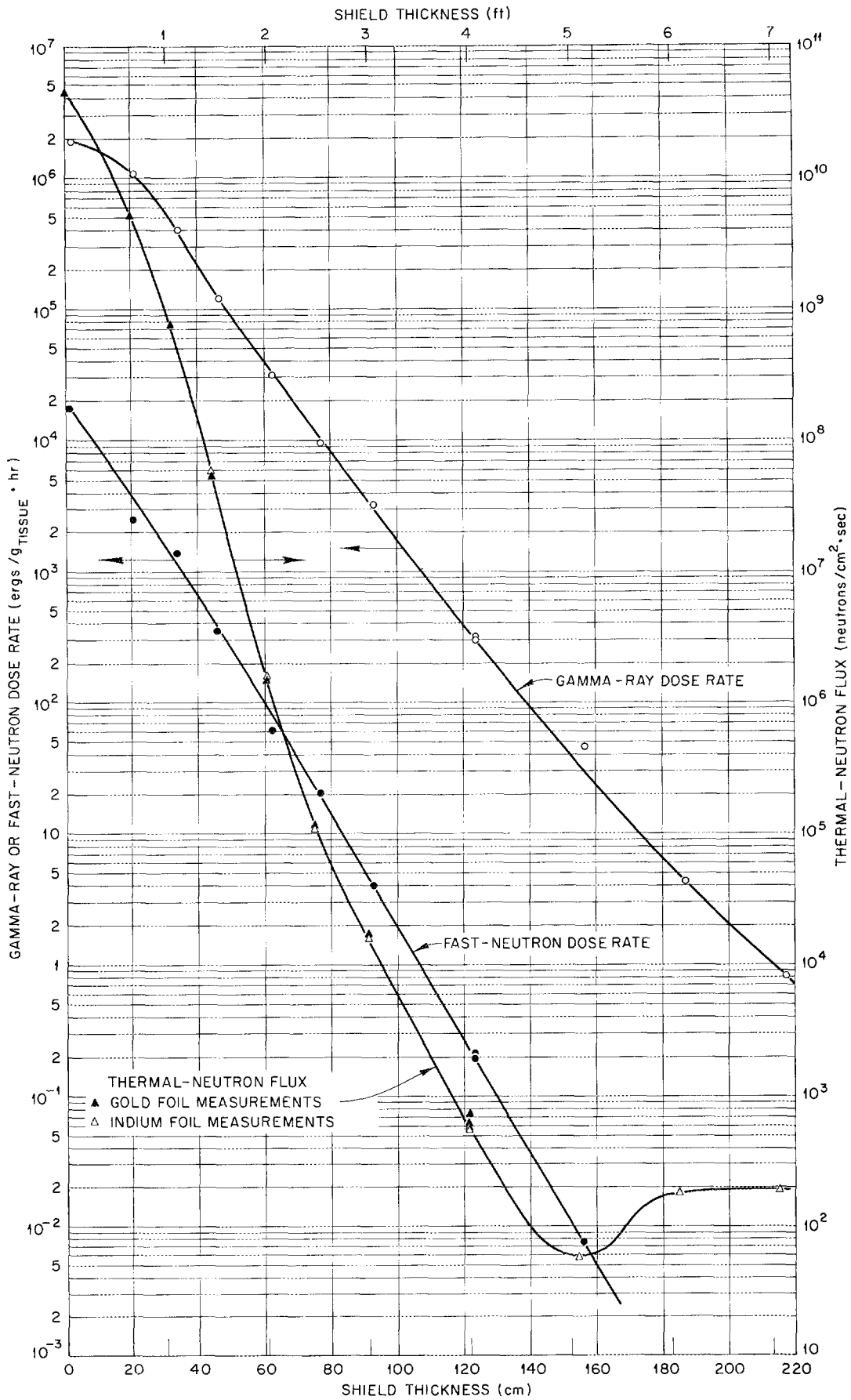


Fig. 6. Gamma-Ray Dose Rate, Fast-Neutron Dose Rate, and Thermal-Neutron Flux as a Function of the Shield Thickness of the ORNL Graphite Reactor Shield.

Table 6. Gamma-Ray Dose Rates as a Function of the Thickness of the ORNL Graphite Reactor Shield

Drilling No.	Shield Thickness ^a		Effective Shield Thickness ^b (cm)	Gamma-Ray Dose Rate (ergs/g _{tissue} ·hr)		
	(ft)	(cm)		Dupont Film	Eastman Film	Ion Chamber
0	7.06	215.3	217.4	1.2×10^0	-	8.1×10^{-1}
1	6.06	184.8	186.9	4.1×10^0	-	4.3×10^0
2	5.06	154.4	156.5	3.19×10^1	-	4.6×10^1
3A	3.99	121.7	123.8	3.23×10^2	-	3.04×10^2
3B	3.99	121.7	123.8	2.90×10^2	-	2.94×10^2
4	2.99	91.1	93.2	3.78×10^3	3.27×10^3	3.25×10^3
5	2.45	74.9	77.0	9.86×10^3	1.15×10^4	9.53×10^3
6	1.98	60.4	62.5	3.52×10^4	3.02×10^4	3.12×10^4
7	1.45	44.2	46.3	1.45×10^5	1.21×10^5	1.20×10^5
8	1.05	32.1	34.2	-	6.58×10^5	4.05×10^5
9	0.62	18.8	20.9	-	1.66×10^6	1.07×10^6
10	0	0	2.1 ^c	-	No Meas.	1.90×10^6

- a. Includes a 2.3-cm thickness of asbestos and two \sim 0.5-cm-thick layers of tar.
 b. Shield thickness extended to include the 2-cm-thick ion chamber wall and the 0.1- and 0.2-cm distance from the wall to the center of detection.
 c. In this case the shield did not include the asbestos layer.

determined after each drilling by measuring the dose rates at various distances back from the bottom of the hole. These gamma-ray traverse measurements are presented in Table 7 and are represented in Fig. 7 by the curves extending to the right of the dose-rate curve for the bottom of the hole.

After the third drilling (shield thickness of 4 ft) it became obvious that the plugs which were serving as shields in the experimental holes adjacent to the hole being drilled were giving rise to a higher gamma-ray dose rate than would be observed in a homogeneous concrete shield (the plugs consisted of 6 ft of graphite, 1 ft of iron-masonite). Therefore, after the third drilling, the graphite-iron-masonite plugs were replaced with close-fitting plugs made of concrete similar to the ordinary and barytes-haydite concrete in the shield. The dose rates at the bottom of the hole and the traverse dose rates were measured both before and after the graphite-iron-masonite plugs were

Table 7. Gamma-Ray Dose Rates Along a Hole in the ORNL Graphite Reactor Shield for Various Distances from the Bottom of the Hole^a

Distance from Bottom of Hole ^a (cm)	Gamma-Ray Dose Rate (ergs/g _{tissue} ·hr)											
	Drilling 0, 215.3-cm Shield	Drilling 1, 184.8-cm Shield	Drilling 2, 154.4-cm Shield	Drilling 3A, 121.7-cm Shield	Drilling 3B, 121.7-cm Shield	Drilling 4, 91.1-cm Shield	Drilling 5, 74.9-cm Shield	Drilling 6, 60.4-cm Shield	Drilling 7, 44.2-cm Shield	Drilling 8, 32.1-cm Shield	Drilling 9, 18.8-cm Shield	Drilling 10, No Shield
2.1	-	4.27 x 10 ⁰	4.58 x 10 ¹	3.04 x 10 ²	2.94 x 10 ²	3.25 x 10 ³	9.53 x 10 ³	3.13 x 10 ⁴	1.20 x 10 ⁵	4.05 x 10 ⁵	-	-
2.13	-	-	-	-	-	-	-	-	-	-	1.07 x 10 ⁶	1.90 x 10 ⁶
2.14	8.00 x 10 ⁻¹	-	-	-	-	-	-	-	-	-	-	-
12.1	-	-	-	2.37 x 10 ²	2.29 x 10 ²	-	6.72 x 10 ³	2.09 x 10 ⁴	-	-	5.96 x 10 ⁵	-
12.9	-	-	-	-	-	2.40 x 10 ³	-	-	-	-	-	-
13.0	-	-	-	-	-	-	5.18 x 10 ³	-	-	-	-	-
17.3	-	-	-	-	-	-	-	-	-	-	-	-
22.1	-	-	-	1.60 x 10 ²	-	-	-	-	-	-	-	-
32.1	-	-	-	1.06 x 10 ²	9.86 x 10 ¹	-	-	-	-	-	-	-
32.6	-	-	-	-	-	9.00 x 10 ²	-	6.83 x 10 ³	2.18 x 10 ⁴	6.64 x 10 ⁴	-	5.22 x 10 ⁵
32.8	-	-	-	-	-	-	-	-	-	-	-	-
42.1	-	-	-	7.4 x 10 ¹	-	-	-	-	-	-	9.23 x 10 ⁴	-
43.4	-	-	-	-	-	-	-	-	-	-	-	-
47.8	-	-	-	-	-	-	1.07 x 10 ³	-	-	-	-	-
52.1	-	-	-	4.9 x 10 ¹	4.49 x 10 ¹	-	-	-	-	-	-	-
52.3	-	-	-	-	-	3.44 x 10 ²	-	-	-	-	-	-
62.1	-	-	-	-	3.19 x 10 ¹	-	-	-	-	-	-	-
63.1	-	-	-	-	-	2.14 x 10 ²	-	1.48 x 10 ³	-	1.27 x 10 ⁴	-	9.11 x 10 ⁴
63.4	-	-	-	-	-	-	-	-	4.45 x 10 ³	-	-	-
67.1	-	-	-	3.33 x 10 ¹	2.82 x 10 ¹	-	-	-	-	-	1.74 x 10 ⁴	-
73.9	-	-	-	2.59 x 10 ¹	2.16 x 10 ¹	-	-	-	-	-	-	-
77.1	-	-	-	-	-	-	2.99 x 10 ²	-	-	-	-	-
78.3	-	-	-	-	-	-	-	-	-	-	-	-
82.1	-	-	-	-	-	9.72 x 10 ¹	-	-	-	-	-	-
87.1	-	-	-	-	1.35 x 10 ¹	-	-	-	-	-	-	-
93.5	-	-	-	-	-	-	-	4.58 x 10 ²	-	-	-	1.36 x 10 ⁴
93.6	-	-	-	-	1.49 x 10 ¹	6.89 x 10 ¹	-	-	-	-	-	-
95.3	-	-	-	-	-	-	-	-	1.31 x 10 ³	3.70 x 10 ³	-	-
104.3	-	-	-	-	-	-	-	-	-	-	5.75 x 10 ³	-
108.8	-	-	-	-	-	-	1.10 x 10 ²	-	-	-	-	-
109.1	-	-	-	-	-	4.85 x 10 ¹	-	-	-	-	-	-
124.0	-	-	-	-	-	-	-	2.08 x 10 ²	-	1.63 x 10 ³	-	6.37 x 10 ³
124.1	-	-	-	-	-	3.35 x 10 ¹	-	-	-	-	-	-
125.8	-	-	-	-	-	-	-	-	5.89 x 10 ²	-	-	-
134.8	-	-	-	-	-	-	-	-	-	-	2.52 x 10 ³	-
139.3	-	-	-	-	-	-	5.61 x 10 ¹	-	-	-	-	-
154.0	-	-	-	-	-	-	-	1.32 x 10 ²	-	-	-	-
154.5	-	-	-	-	-	-	-	-	-	8.60 x 10 ²	-	2.83 x 10 ³
165.3	-	-	-	-	-	-	-	-	-	6.88 x 10 ²	1.40 x 10 ³	-
169.8	-	-	-	-	-	-	-	-	-	-	-	-
171.2	-	-	-	-	-	-	-	-	2.99 x 10 ²	-	-	1.66 x 10 ³
182.9	-	-	-	-	-	-	-	-	-	-	-	-
183.9	-	-	-	-	-	-	-	-	-	5.71 x 10 ²	-	1.30 x 10 ³
199.4	-	-	-	-	-	-	-	-	-	-	-	-

a. Includes the 2-cm-thick ion chamber wall and the 0.1- to 0.2-cm-thick distance from the wall to the center of detection.

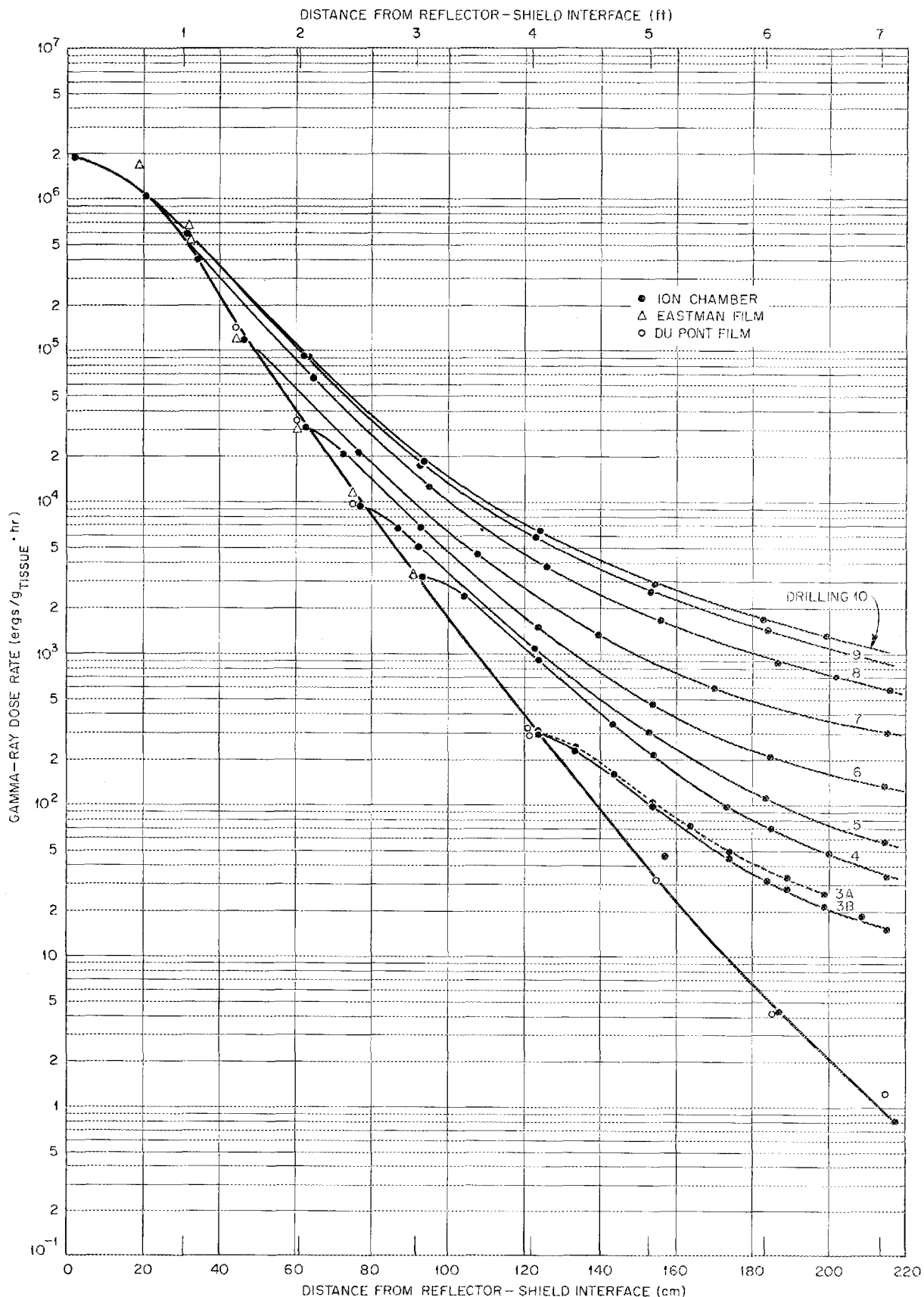


Fig. 7. Gamma-Ray Dose Rate Along Hole in ORNL Graphite Reactor Shield as a Function of the Distance from the Reactor-Shield Interface. A concrete plug was placed between detector and outside face of shield. Heavy line represents dose rate as a function of shield thickness.

replaced by the concrete plugs. Measurements for Drilling 3A, represented by the dashed traverse curve in Fig. 6, were made before the graphite-iron-masonite plugs were removed, and the measurements for Drilling 3B were made after they had been replaced with the concrete plugs. Dose rates with the graphite-iron-masonite plugs inserted were greater than those with concrete plugs by 3% at the bottom of the hole, increasing to about 20% near the outside of the hole. Measurements taken during Drilling 5 (shield thickness of 2-1/2 ft) may have been affected in a similar manner by the temporary replacement of the concrete plugs in a nearby experimental hole (Hole 15) with an experimental graphite-iron-masonite plug during a normal weekly shutdown. However, this experimental plug was replaced by the concrete plugs for the remainder of the experiment.

Personnel Monitoring Film Measurements

The gamma-ray dose rates measured by the gamma-sensitive films (supplied by the ORNL Health Physics Division) were determined by comparing the opacity of the films on a densitometer with films which had been exposed to known gamma-ray dose rates. The film measurements were less accurate than those made with the ion chamber, but they were valuable for purposes of comparison.

DuPont 552 dosimeter film packets, each of which contained one DuPont "sensitive" film No. 502, were used to measure the dose rates below 1 r/hr ($93 \text{ ergs/g}_{\text{tissue}} \cdot \text{hr}$) for shield thicknesses from 7 to 1.5 ft. The results are included in Table 6. Insensitive films were used to measure the higher dose rates for these shield thicknesses. The results were surprisingly close to the ion chamber measurements even well above the reported range of the film ($< 50 \text{ r/hr}$).

High-range Eastman 5308 films, reported to be accurate up to 1000 r/hr, were used for shield thicknesses from 3 to 0.6 ft. Doses measured with these films are also given in Table 6.

When placed in the hole all film detectors were followed by a 14-in.-long concrete plug constructed from the same type of concrete as that in which the measurements were being made. For the measurements in the Portland concrete near the reflector this 14-in. plug was backed up by a 5-ft barytes-haydite concrete plug.

Ionization Chamber Measurements

The 50-cc ionization chamber, which has been described elsewhere,⁶ was used to measure dose rates at all shield thicknesses, although for the final measurement, that is, the measurement at the reflector-shield interface, it was necessary to reduce the reactor power to 50 kw so that the observed dose rate would still be within the operating range of the instrument. This final measurement was normalized to full power by the ratio of the saturated activities of gold foils (1 cm² by 5 mils thick) exposed at both power levels.

When placed in the hole, the ion chamber occupied a space equal to the diameter of the hole and 4 in. long. The concrete plugs described above were placed immediately behind the chamber and electrical leads to the ion chamber were passed through an axial hole in each plug.

The ionization chamber was connected to a modified Q826 electrometer⁷ and was operated at room temperature with a 10-psi carbon dioxide gas pressure. Under these conditions a potential of 570 volts between the collecting electrode and ground was sufficient to assure operation of the chamber in the ionization region for all gamma-ray dose rates measured.

The gamma-ray dose rate was proportional to the ionization current which flowed through the variable megohm grid resistor of the input electrometer triode. The resulting grid voltage produced an unbalance in an electrometer bridge circuit which was then exactly cancelled by a known bucking voltage to give a null condition on a galvanometer.

The gamma-ray dose rate was determined from the reference bucking voltage by calibrating the ion chamber with a known gamma-ray dose rate. A Co⁶⁰ source for which the dose rate was known (to within $\pm 5\%$) was placed at several distances from the ion chamber, and the bucking voltage, V_k , was recorded. The dose at the chamber, D_k , was calculated using inverse square attenuation. The unknown dose in the shield, D_u , was then determined from the proportionality,

$$\frac{D_u}{V_u} = \frac{D_k}{V_k}$$

-
6. L. H. Ballweg, J. L. Meem, "A Standard Gamma Ray Ionization Chamber for Shielding Measurements," ORNL-1028 (1951).
 7. F. M. Glass, "A Simple Low Drift Electrometer," Nucleonics 10, No. 2, 36 (1952).

where V_u is the bucking voltage for the unknown dose. Measurements were made using electrometer grid resistances of 10^7 , 10^8 , 10^9 , 10^{10} , and 10^{11} ohms and the results were averaged to give the reported dose.

The response of the counter was estimated by the following equation:⁶

$$\text{Dose Rate (r/hr)} = \frac{E}{IV_o \left(\frac{P}{29.92} \right) \left(\frac{273}{T_o} \right) R}$$

where

E = volts (reference voltage),

V_o = volume of chambers, cm^3 ,

$\frac{273}{T_o}$ = temperature correction, $^{\circ}\text{K}$,

P = CO_2 pressure in chamber, inches of Hg,

$\frac{1}{29.92}$ = pressure correction,

R = value of variable resistor, ohms,

I = ionization current which will be produced by 1 r/hr in 1 cc of CO_2 gas at standard temperature and pressure
 $= 1.438 \times 10^{-13}$ amp/cc.

When substituting the value V_k in the equation as determined from the Co^{60} source, it was found that the chamber gives a lower dose-rate reading than the calculated dose rate in regions up to 20 to 30 mr/hr. However, above this dose rate the estimated and measured dose rates were within experimental statistics.

The position of the center of detection of the ion chamber was determined by the method derived by Hungerford,⁸ in which it was assumed that the gamma radiation was 75% collimated and 25% isotropic at each shield thickness. The approximate position of the center of detection for the ion chamber was 2.1

8. H. E. Hungerford, "Center of Detection Calculations for Neutron Counters and Ion Chambers," ORNL-CF-51-5-177 (1951).

to 2.2 cm from the front of the outer case. For the traverse measurements at a particular shield thickness, the center of detection was assumed to be equal to that calculated for the measurement at the bottom of the hole.

Fast-Neutron Dose Rates

The fast-neutron dose rates were measured as a function of shield thickness by means of a proton-recoil dosimeter.^{9,10} The results are presented in Table 8 and Fig. 8. As for the gamma-ray measurements, dose rates due to fast neutrons streaming down the hole were also determined by taking measurements at various distances back from the bottom of the hole for each shield thickness.

Table 8. Fast-Neutron Dose Rates as a Function of the Thickness of the ORNL Graphite Reactor Shield

Drilling No.	Shield Thickness ^a		Effective Shield Thickness ^b (cm)	Fast-Neutron Dose Rate (ergs/g _{tissue} ·hr)
	(ft)	(cm)		
0	7.06	215.3	216.8	Not detectable
1	6.06	184.8	186.3	Not detectable
2	5.06	154.4	156.0	7.7×10^{-3}
3A	3.99	121.7	123.4	1.93×10^{-1}
3B	3.99	121.7	123.4	2.12×10^{-1}
4	2.99	91.1	92.9	4.12×10^0
5	2.45	74.9	76.7	2.06×10^1
6	1.98	60.4	62.1	6.17×10^1
7	1.45	44.2	45.9	3.55×10^2
8	1.05	32.1	33.8	1.40×10^3
9	0.62	18.8	20.4	2.49×10^3
10	0	0	1.6	1.78×10^4

a. Includes a 2.3-cm thickness of asbestos and two ~0.5-cm-thick layers of tar.

b. Shield thickness extended to include the 0.5-cm wall thickness and 0.8- to 1.1-cm distance from the front wall of the dosimeter to its center of detection.

The results of these traverse measurements are given in Table 9 and are

9. G. S. Hurst, R. S. Ritchie, and H. N. Wilson, "A Count-Rate Method of Measuring Fast Neutron Tissue Dose," Rev. Sci. Instr., 22, 981 (1951).
10. G. S. Hurst, "An Absolute Tissue Dosimeter for Fast Neutrons," Brit. J. Radiol. XXVII, No. 318, 353 (1954).

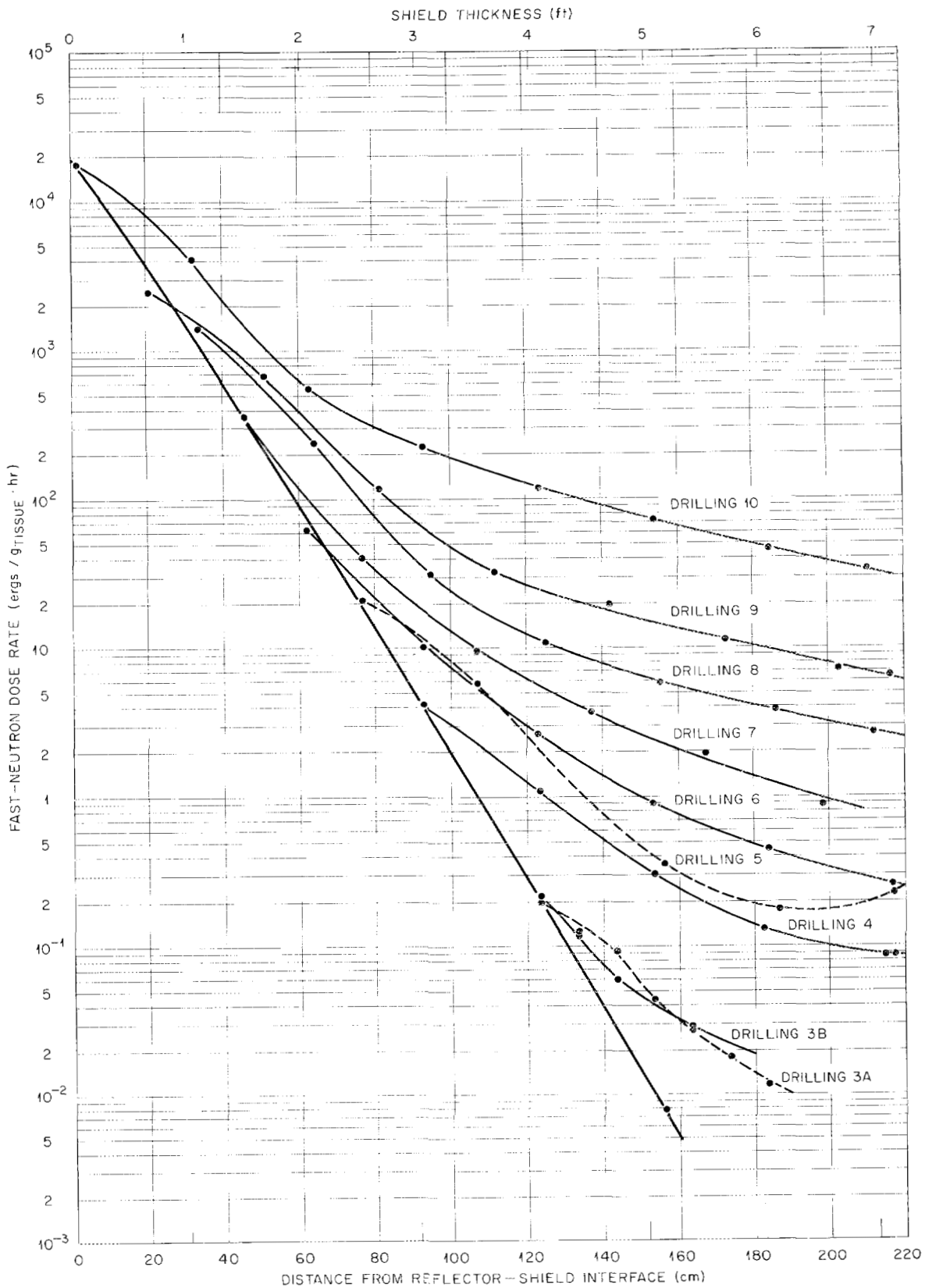


Fig. 8. Fast-Neutron Dose Rate Along Hole in ORNL Graphite Reactor Shield as a Function of the Distance from the Reactor-Shield Interface. A concrete plug was placed between detector and outside face of shield. Heavy line represents dose rate as a function of shield thickness.

Table 9. Fast-Neutron Dose Rates Along a Hole in the ORNL Graphite Reactor Shield for Various Distances from the Bottom of the Hole^a

Distance from Bottom of Hole ^a (cm)	Fast-Neutron Dose Rate (ergs/g _{tissue} ·hr)											
	Drilling 0, 215.3-cm Shield	Drilling 1, 184.8-cm Shield	Drilling 2, 154.4-cm Shield	Drilling 3A, 121.7-cm Shield	Drilling 3B, 121.7-cm Shield	Drilling 4, 91.1-cm Shield	Drilling 5, 74.9-cm Shield	Drilling 6, 60.4-cm Shield	Drilling 7, 44.2-cm Shield	Drilling 8, 32.1-cm Shield	Drilling 9, 18.3-cm Shield	Drilling 10, No Shield
1.6	-	-	7.7 x 10 ⁻³	-	-	-	-	-	-	-	-	-
1.7	-	-	-	1.93 x 10 ⁻¹	2.12 x 10 ⁻¹	-	-	-	-	-	-	1.78 x 10 ⁴
1.8	-	-	-	-	-	4.12	2.06 x 10 ¹	6.17 x 10 ¹	3.55 x 10 ²	1.40 x 10 ³	-	-
11.7	-	-	-	1.21 x 10 ⁻¹	1.17 x 10 ⁻¹	-	-	-	-	-	-	-
21.8	-	-	-	9.11 x 10 ⁻²	-	-	-	-	-	-	-	-
22.1	-	-	-	-	5.86 x 10 ⁻²	-	-	-	-	-	-	-
31.7	-	-	-	4.23 x 10 ⁻²	-	-	-	-	-	-	-	-
32.1	-	-	-	-	-	-	-	-	-	-	-	-
32.2	-	-	-	-	-	-	-	-	-	-	-	-
32.3	-	-	-	-	-	1.07	5.67	9.98	4.20 x 10 ¹	2.36 x 10 ²	6.97 x 10 ²	4.11 x 10 ³
41.7	-	-	-	2.73 x 10 ⁻²	2.79 x 10 ⁻²	-	-	-	-	-	-	-
51.7	-	-	-	1.73 x 10 ⁻²	-	-	-	-	-	-	-	-
61.7	-	-	-	1.13 x 10 ⁻²	-	-	-	-	-	-	-	-
62.6	-	-	-	-	-	-	-	-	-	-	-	-
62.7	-	-	-	-	-	-	-	2.56	9.39	3.12 x 10 ¹	1.16 x 10 ²	5.53 x 10 ²
62.8	-	-	-	-	-	2.99 x 10 ⁻¹	-	-	-	-	-	-
81.4	-	-	-	-	-	-	3.49 x 10 ⁻¹	-	-	-	-	-
93.0	-	-	-	-	-	-	-	-	-	-	-	-
93.1	-	-	-	-	-	-	-	8.78 x 10 ⁻¹	3.62	1.05 x 10 ¹	3.17 x 10 ¹	2.22 x 10 ²
93.3	-	-	-	-	-	1.25 x 10 ⁻¹	-	-	-	-	-	-
111.9	-	-	-	-	-	-	1.70 x 10 ⁻¹	-	-	-	-	-
123.5	-	-	-	-	-	-	-	-	-	-	1.89 x 10 ¹	-
123.6	-	-	-	-	-	-	-	4.31 x 10 ⁻¹	1.87	5.67	-	1.15 x 10 ²
123.8	-	-	-	-	-	8.30 x 10 ⁻²	-	-	-	-	-	-
126.6	-	-	-	-	-	8.33 x 10 ⁻²	-	-	-	-	-	-
142.4	-	-	-	-	-	-	2.18 x 10 ⁻¹	-	-	-	-	-
154.0	-	-	-	-	-	-	-	-	-	-	1.09 x 10 ¹	-
154.1	-	-	-	-	-	-	-	-	8.50 x 10 ⁻¹	3.76	-	7.0 x 10 ¹
156.5	-	-	-	-	-	-	-	2.50 x 10 ⁻¹	-	-	-	-
180.0	-	-	-	-	-	-	-	-	-	2.60	-	-
184.5	-	-	-	-	-	-	-	-	-	-	6.90	4.45 x 10 ¹
197.9	-	-	-	-	-	-	-	-	-	-	6.22	-
210.5	-	-	-	-	-	-	-	-	-	-	-	3.24 x 10 ¹

a. Includes the 0.5-cm-thick dosimeter wall and the 0.8- to 1.1-cm distance from the wall to the center of detection.

represented in Fig. 8 by curves extending to the right of the dose-rate curve for the bottom of the hole. Shield thicknesses again include, in addition to the concrete, the 2.3-cm-thick layer of asbestos, the water-proofing tar coatings, and the distance from the front to the center of detection of the dosimeter (~ 1 cm).

The presence of the graphite-iron-masonite plugs referred to previously also affected the fast-neutron measurements for Drillings 3A and 5, as indicated by the dashed lines in Fig. 8. The effect on the measurements for Drilling 3A can be determined by a comparison with those for Drilling B, in which case the graphite-iron-masonite plugs were replaced with concrete plugs. For shield thicknesses less than 3 ft dosimeter measurements were made at a reduced reactor power level in order to reduce the gamma radiation, so that gamma-ray (pile-up) pulses would not alter the response of the counter. The results were normalized to full power by determining the ratio of the saturation activities of standard gold foils irradiated both at the reduced and at full power.

When placed in the drilled hole, the dosimeter fit snugly into a recess in the end of the 14-in.-long Portland or barytes-haydite concrete plug, the recess being exactly as deep as the length of the dosimeter. At the outer end of the concrete plug was the preamplifier (cathode follower) which also fit snugly into a recess in the plug and which was connected to the dosimeter by shielded leads passing axially through the plug. For the smaller shield thicknesses the plug housing the dosimeter and preamplifier was backed by a 5-ft-long barytes-haydite concrete plug.

The dosimeter used was the two-chamber type developed by Hurst, Ritchie, and Wilson.⁹ It consists of a brass cylinder about 2 in. in diameter and 5 in. long. Running the length of the axis of the cylinder is a 0.002-in.-dia stainless steel wire, maintained at a positive potential of approximately 2000 volts above the grounded cylinder. The cylinder is divided into two chambers of equal volume to improve the sensitivity of the counter. Each chamber contains ethylene gas at atmospheric pressure. The inner surface of the cylinder is lined with a 1/8-in.-thick coating of polyethylene which

corresponds in molecular composition to the ethylene gas in the chambers, thus approaching a true Bragg-Gray cavity.

Since the dosimeter is operated as a proportional counter, the size of the voltage pulse resulting from a neutron-proton collision is proportional to the amount of energy dissipated in the gas.

The pulse from the dosimeter was fed to a preamplifier (cathode follower), then to an A-1 amplifier, and finally recorded by means of a scaler.

The response of the dosimeter to gamma rays (Fig. 9) was determined by placing the dosimeter in a known gamma-ray flux emitted by a Co^{60} source and discriminating at a level which excludes the gamma-ray pulses. Thus, some of the proton-recoil pulses fall below the discrimination level and are not counted, but this loss is estimated when extrapolating the pulse-height curve to zero.

The response of the dosimeter to neutrons was determined at the preset gamma-ray bias level using a Po-Be source of known strength. Since the source strength was known in terms of neutrons per square centimeter per second, a conversion factor of $0.174 \text{ (ergs/g}\cdot\text{hr)}/(\text{neutrons/cm}^2\cdot\text{sec})$ (determined by comparing the Po-Be source spectrum with the first-collision dose curve for tissue and ethylene¹¹) was used to express the dosimeter measurement in terms of dose rate. In order to calibrate the dosimeter, a plot of the log counts per minute versus the pulse-height selector (PHS) was obtained with the Po-Be source.

The total area under the integral (PHS) curve, which is proportional to the dose rate, was estimated by extrapolating the curve to PHS equal zero.

The unknown dose rates were computed from the proportionality,

$$\frac{\text{Po-Be source dose rate}}{\text{Area for Po-Be source}} = \frac{\text{Unknown dose rate}}{\text{Area for unknown dose in shield}}$$

To maintain a valid proportionality between the known and unknown dose rates, the gamma-ray preset bias level was not exceeded when the measurements were made in the shield. The dosimeter was calibrated before each series of measurements.

11. T. V. Blosser, "Applied Nuc. Phys. Div. Ann. Rep., Sept. 10, 1956," ORNL-2081, p. 151.

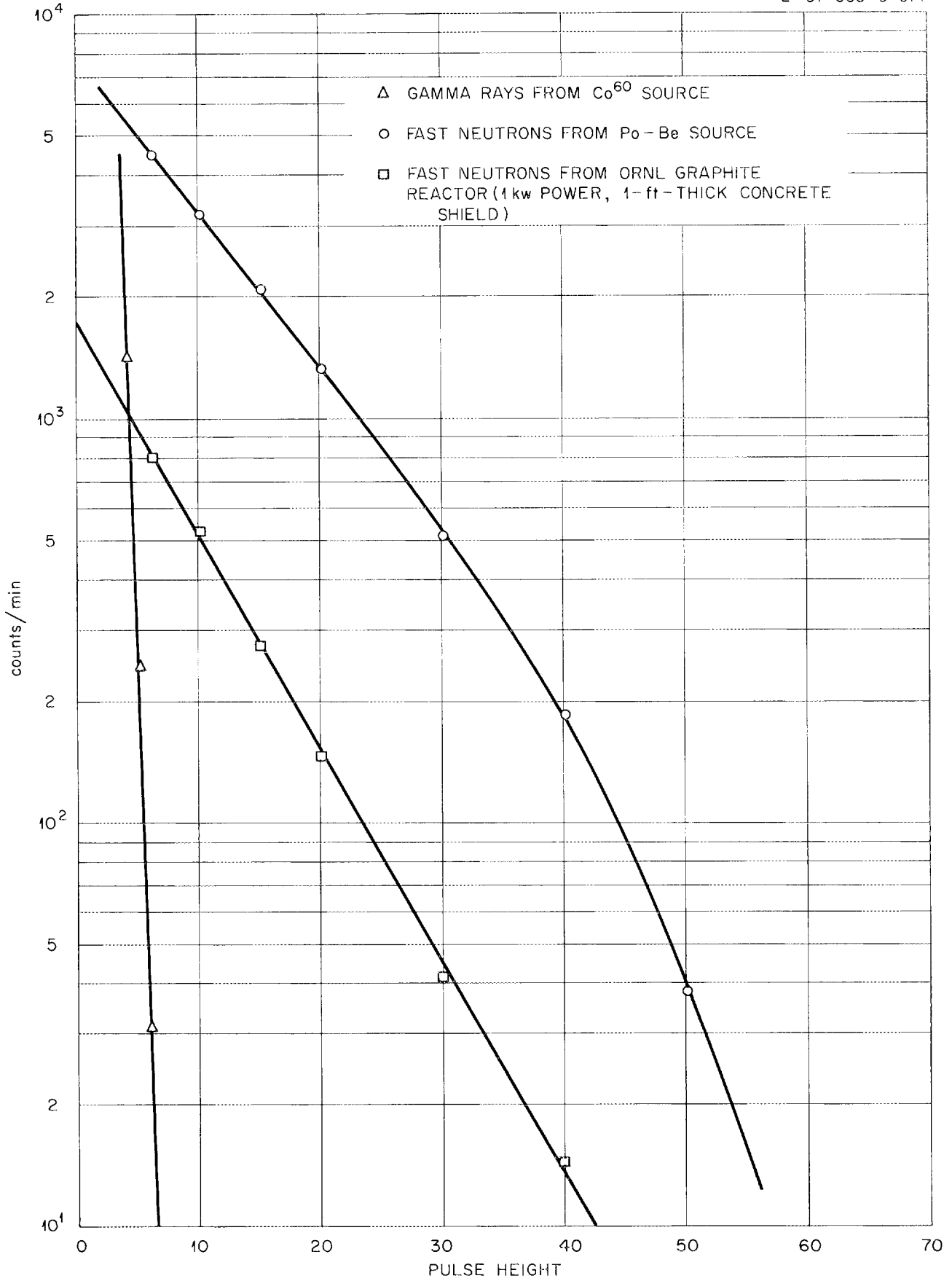


Fig. 9. Response of Fast-Neutron Dosimeter to Mixed Radiation.

The position of the center of detection of the fast-neutron dosimeter was determined by the method derived by Hungerford.⁸ The assumptions used for these calculations were the same as those for the ion chamber center-of-detection calculations. The wall thickness of the dosimeter is 0.5 cm and the distance from the front of the counter to the center of detection varied from 0.8 to 1.1 cm.

Thermal-Neutron Flux Measurements

Foil Measurements

The thermal-neutron flux at each drilling depth was calculated from the activities of bare and cadmium-covered gold and indium foils exposed at the bottom of the hole. Gold foils were used for measurements at shield thicknesses of less than 4 ft, while the indium foils were used for thicknesses from 7 to 1-1/2 ft. The resulting thermal-neutron fluxes are presented in Table 10 and plotted as a function of the shield thickness in Figs. 6 and 10. Also included in Table 10 are cadmium ratios measured for both gold and indium foils.

Table 10. Thermal-Neutron Fluxes and Cadmium Ratios as a Function of the Thickness of the ORNL Graphite Reactor

Drilling No.	Shield Thickness		Thermal-Neutron Flux (neutrons/cm ² .sec)		Cadmium Ratio	
	(ft)	(cm)	Gold Foils	Indium Foils	Gold Foils	Indium Foils
	0	7.06	215.3	-	1.88×10^2	-
1	6.06	184.8	-	1.78×10^2	-	14.3
2	5.06	154.4	-	0.578×10^2	-	9.21
3A	3.99	121.7	7.43×10^2	6.03×10^2	-	6.94
3B	3.99	121.7	6.26×10^2	5.85×10^2	4.75	7.30
4	2.99	91.1	1.75×10^4	1.66×10^4	8.00	13.1
5	2.45	74.9	1.13×10^5	1.10×10^5	12.50	12.0
6	1.98	60.4	1.48×10^6	1.51×10^6	34.80	48.6
7	1.45	44.2	5.27×10^7	5.71×10^7	34.95	63.2
8	1.05	32.1	7.47×10^8	-	187.5	-
9	0.62	18.8	5.17×10^9	-	197.5	-
10	0	0	4.47×10^{10}	-	174.1	-

The values of the thermal-neutron fluxes for Drillings 3A and 3B as measured by gold foils are not as accurate as those measured by the indium foils because the cadmium-covered gold foil activity was only slightly above background. The increase in the thermal-neutron flux near the outside of the shield is believed to be caused by the normal thermal-neutron background outside the shield.

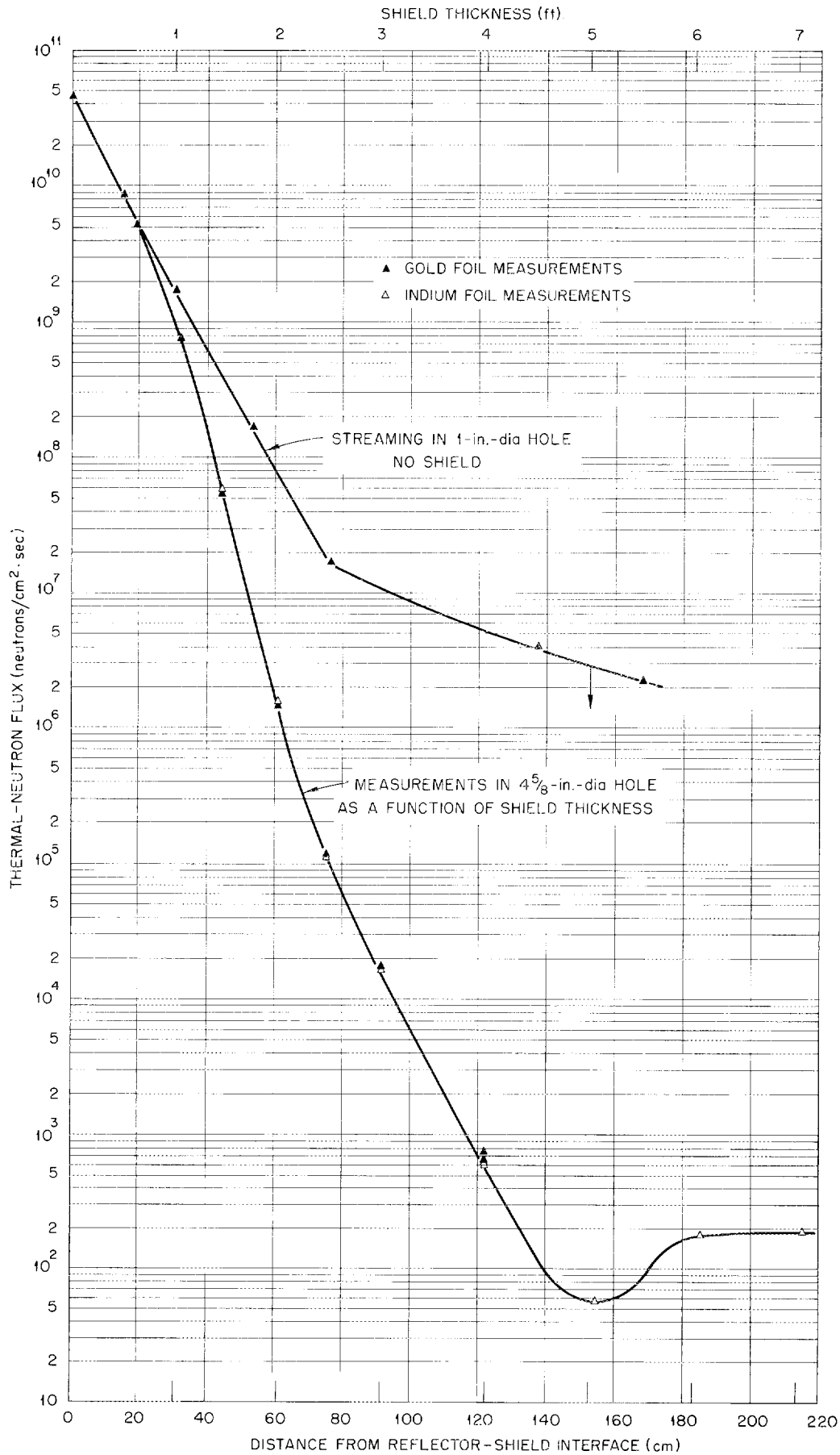


Fig.10. Thermal-Neutron Flux in 4 5/8-in.-dia and 1-in.-dia Holes in the ORNL Graphite Reactor Shield. A concrete plug was placed between detector and outside face of shield.

The "standard" indium foils used for these measurements were cut with a 25-cm² rectangular die from large indium sheets 5 mils thick. "Standard" gold foils were 1-cm² squares, 5 mils thick. The foils were cleaned with distilled water and then with acetone, after which they were weighed. Variations in the weights were less than 4%. The term "standard" foil refers to the size of foil which was calibrated in the ORNL Standard Pile. This calibration is discussed further below.

Foils were irradiated one at a time by attaching a single foil to the end of a concrete plug and inserting the plug into a hole. Bare foils were protected from foreign contamination by 20-mil-thick aluminum covers. The cadmium covers used in obtaining the resonance activation were 30 mils thick.

Both sides of the irradiated foils were counted on two Model O-799 ORNL gas-flow beta proportional counters. Results obtained from the two counters were averaged.

In order to determine the thermal-neutron streaming data a 1-in.-dia axial hole was drilled in a 7-ft-long concrete plug which was inserted in the original 4-5/8-in.-dia hole. The concrete in the plug matched the type of concrete in the shield. Gold foils, both bare and cadmium covered, were attached to the inner end of a 1-in.-dia concrete plug which was made to fit in the axial hole of the larger concrete plug. This 1-in.-dia plug was encased in aluminum. The 1-in.-dia hole rather than the 4-5/8-in.-dia hole was used for the streaming measurements both to decrease the biological hazard during foil exposures and to decrease the time necessary to insert and withdraw the foils because of the greater ease in handling the smaller plug. The results of the streaming measurements are given in Table 11 and included on Fig. 10.

Table 11. Thermal-Neutron Fluxes Along a 1-in.-dia Hole in the ORNL Graphite Reactor Shield for Various Distances from the Bottom of the Hole

Distance from Bottom of Hole		Thermal-Neutron Flux (neutrons/cm ² ·sec)	Cadmium Ratio
(ft)	(cm)		
0	0	4.47 x 10 ¹⁰	174
0.5	15.2	8.71 x 10 ⁹	153
1.0	30.5	1.67 x 10 ⁹	73.4
1.75	53.3	1.64 x 10 ⁸	247
2.5	76.2	1.66 x 10 ⁷	127
4.5	137	3.97 x 10 ⁶	127
5.5	168	2.30 x 10 ⁶	140

Calculation of the Flux from the Foil Measurements

A quantity (henceforth referred to as an activity) proportional to the true saturated foil activity was calculated for each side of each exposed foil from the relation

$$A = k\lambda N \left(\frac{1}{1 - e^{-\lambda t_1}} \right) \left(\frac{1}{e^{-\lambda t_2}} \right) \left(\frac{1}{1 - e^{-\lambda t_3}} \right)$$

where

A = quantity proportional to the saturated activity, counts/min,

k = counter factor checked periodically during the present investigation,

λ = decay constant, min^{-1} ,

N = net counts in time t_3 ,

t_1 = exposure time, min,

t_2 = wait time, min,

t_3 = count time, min.

The calculated activity, A, for each side of the foil was averaged.

The activity resulting from the irradiation of the bare foil was the sum of the activities caused both by thermal neutrons and by resonance neutrons, i.e., neutrons of energy greater than thermal. Activation essentially by resonance neutrons alone was obtained from the cadmium-covered foils. It was necessary to multiply the resonance activity measured using indium foils by 1.14 in order to account for resonance-neutron absorption by the 30-mil-thick cadmium cover.^{12,13} A similar correction for cadmium-covered gold foils was unnecessary since its resonance energy (5 ev) is considerably higher than that for indium (1.4 ev). The saturated thermal activity for indium foils was, therefore, obtained from the differences between the activity for the

-
12. G. S. Hurst, J. A. Harter, P. N. Hensley, W. A. Mills, M. Slater, P. W. Reinhardt, "Techniques of Measuring Neutron Spectra with Thermal Detectors - Tissue Dose Determination," *Rev. Sci. Instr.* 27, 153 (1956).
 13. D. J. Hughes, "Pile Neutron Research," Addison-Wesley Publishing Co., Cambridge, Mass. (1953).

bare foils and 1.14 times the activity for the cadmium-covered foils, while the thermal activity for the gold foils was obtained simply from the difference between activities of the bare and cadmium-covered foils.

Phenomena such as internal beta absorption, self-protection, hardening, obliquity, and flux depression prevent the use of the simple relation for the flux,

$$\phi_{th} = A_{th}/\Sigma$$

where A_{th} is the true saturated thermal activity and Σ is the macroscopic activation cross section. Although corrections for each of these phenomena may be approximated, they can be taken into account more accurately by "calibrating" standard foils in a known thermal-neutron flux. Empirical proportionality factors between the measured activity and the thermal-neutron flux, which include the macroscopic cross section, Σ , as well as the corrections for the phenomena mentioned above, have been determined with the ORNL Standard Pile for the gold and indium standard foils used in the present investigation and are equal to 3.29 and 0.0617 for gold and indium, respectively, when these foils are counted in the beta proportional counters mentioned above.¹³

It was necessary to make a further correction for flux depression since the standard foil calibration was made in a graphite medium (Standard Pile) and the foils for the present investigation were exposed in a concrete medium (reactor shield) and the flux is depressed differently in the two mediums. This depression was assumed to be significant for the indium foils only since the gold foils were so small.

The procedure used to determine the relative flux depression by the indium foils in concrete and graphite was the same as that used by Klema and Ritchie^{14, 15} to determine the ratio between water and graphite. As the thickness of a foil approaches zero, the flux depression caused by that foil

14. E. B. Johnson and J. L. Meem, "Determination of Power of the Bulk Shielding Reactor, Part II," ORNL-1438, Appendix D (1953).

15. E. D. Klema and R. H. Ritchie, "Preliminary Report on Determination of the Thermal Neutron Flux in Water," ORNL-CF-51-4-103 (1951).

will approach zero. If the specific saturated activity (counts per minute per gram) becomes A_0 in the limit as the foil thickness approaches zero, and if the specific saturated activity of a 5-mil-thick standard foil is represented by A_5 , the ratio A_0/A_5 will be proportional to the flux depression caused by the presence of the standard foil. The ratio of the flux depression in concrete to that in graphite, R , can then be expressed as $R = (A_0/A_5)_{\text{concrete}} / (A_0/A_5)_{\text{graphite}}$. For convenience, this may be further expressed as $R = (A_0/A_1)_{\text{concrete}} (A_1/A_5)_{\text{concrete}} / (A_0/A_1)_{\text{graphite}} (A_1/A_5)_{\text{graphite}}$. The factors A_1/A_5 were determined experimentally; the factors A_0/A_1 were calculated.

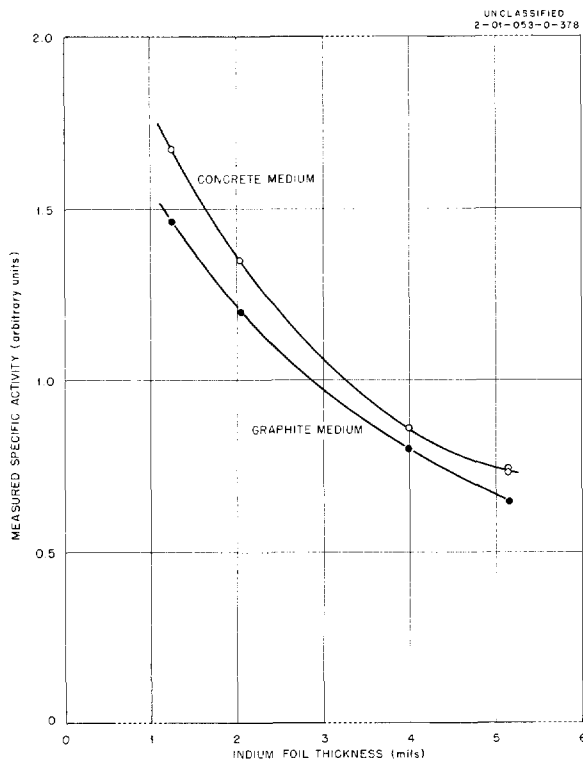


Fig 11. Specific Thermal-Neutron Activity of Indium Foils as a Function of the Foil Thickness.

The factors A_1/A_5 were determined from the irradiations of indium foils, varying in thickness from 1 to 5 mils, in both a graphite medium (ORNL Standard Pile, Slot 3) and a concrete medium (in barytes-haydite concrete, at a shield thickness of 2-1/2 ft). A quantity proportional to the specific thermal saturation activity of each foil was determined by irradiating both bare and cadmium-covered foils. The experimental results are listed in Table 12 and the measured specific activities are plotted as a function of the indium foil thickness in Fig. 11. From the two curves, the following ratio was determined:

$$\frac{(A_1/A_5)_{\text{concrete}}}{(A_1/A_5)_{\text{graphite}}} = \frac{2.44}{2.37} = 1.03$$

It should be noted that the true values for A_1/A_5 are not represented by the numbers 2.44 and 2.37 since internal

Table 12. Measured Saturated and Specific Thermal Activities of Indium Foils in Concrete and Graphite Mediums

Foil Thickness (mils)	Foil Weight (g)	Measured Saturated Activity (counts/min)		Specific Activity (counts min ⁻¹ /g)	
		In Concrete	In Graphite	In Concrete	In Graphite
5.147	2.3863	1.736 x 10 ⁶	1.536 x 10 ⁵	7.275 x 10 ⁶	6.44 x 10 ⁴
		1.763 x 10 ⁶		7.388 x 10 ⁶	
3.985	1.8460	1.580 x 10 ⁶	1.476 x 10 ⁵	8.559 x 10 ⁶	8.00 x 10 ⁴
2.047	0.9483	1.282 x 10 ⁶	1.133 x 10 ⁵	1.352 x 10 ⁷	1.195 x 10 ⁵
1.259	0.5828	9.77 x 10 ⁵	8.54 x 10 ⁴	1.676 x 10 ⁷	1.465 x 10 ⁵

beta absorption, self protection, etc. have not been taken into account. However, in the ratio of the two above numbers, the effects of these phenomena do cancel out.

The validity of extrapolating the curves in Fig. 11 to zero thickness is questionable so a theoretical method for determining the ratios A_0/A_1 developed by Skyrme¹⁶ was used. Skyrme's method is based on transport theory and applies to plane foils of finite radius. Nuclear constants for the concrete were determined from the chemical analysis and water content for Drilling 5 (shield thickness of 2-1/2 to 3 ft) given in Tables 1 and 3. The factors A_0/A_1 determined by Skyrme's method are

$$\frac{(A_0/A_1)_{\text{concrete}}}{(A_0/A_1)_{\text{graphite}}} = \frac{1.034}{1.021} = 1.013$$

The ratio of flux depression by a standard indium foil in concrete to that in graphite is, therefore,

$$R = \frac{(A_0/A_5)_{\text{concrete}}}{(A_0/A_5)_{\text{graphite}}} = (1.03)(1.013) = 1.04$$

16. T. H. R. Skyrme, MS-91 (Classified).

The final expression used to obtain the thermal-neutron flux from gold and indium foil activities can then be written as

$$\phi_{\text{th}_{\text{Au}}} = 3.29 (A_{\text{Bare}} - A_{\text{Cd-covered}})$$

$$\phi_{\text{th}_{\text{In}}} = 0.0617 (1.04) (A_{\text{Bare}} - 1.14 A_{\text{Cd-covered}})$$

Appendix A

LIST OF TABLES

<u>Table No.</u>		<u>Page No.</u>
1	Chemical Analysis (Dry Basis) of Samples of Concrete from the ORNL Graphite Reactor Shield	8
2	Spectrographic Analysis of Samples of Concrete from the ORNL Graphite Reactor Shield	9
3	Water Content, Density, and Compressive Strength of Samples of Concrete from the ORNL Graphite Reactor Shield	7
4	Decay of Gamma-Ray Activity in Samples of Concrete from the ORNL Graphite Reactor Shield	12
5	Temperature Gradient Throughout the ORNL Graphite Reactor Shield	13
6	Gamma-Ray Dose Rates as a Function of the Thickness of the ORNL Graphite Reactor Shield	16
7	Gamma-Ray Dose Rates Along a Hole in the ORNL Graphite Reactor Shield for Various Distances from the Bottom of Hole	18
8	Fast-Neutron Dose Rates as a Function of the Thickness of the ORNL Graphite Reactor Shield	23
9	Fast-Neutron Dose Rates Along a Hole in the ORNL Graphite Reactor Shield for Various Distances from the Bottom of the Hole	25
10	Thermal-Neutron Fluxes and Cadmium Ratios as a Function of the Thickness of the ORNL Graphite Reactor .	29
11	Thermal-Neutron Fluxes Along a 1-in.-dia Hole in the ORNL Graphite Reactor Shield for Various Distances from the Bottom of the Hole	31
12	Measured Saturated and Specific Thermal Activities of Indium Foils in Concrete and Graphite Mediums . . .	35

Appendix B

LIST OF FIGURES

<u>Fig. No.</u>		<u>Page No.</u>
1	Cross Section of ORNL Graphite Reactor Shield	1
2	Relative Location of 4-5/8-in.-dia Hole with Respect to Adjacent Experimental Holes on South Face of ORNL Graphite Reactor	4
3	Core Drilled from Outside Foot of ORNL Graphite Reactor Shield	6
4	Decay of Activity in the Concrete Samples Removed from the ORNL Graphite Reactor Shield After Each Core Drilling .	11
5	Temperature Gradient Throughout ORNL Graphite Reactor Shield During 3500-kw Operation and 5 and 10 hr After Shutdown	14
6	Gamma-Ray Dose Rate, Fast-Neutron Dose Rate, and Thermal-Neutron Flux as a Function of the Shield Thickness of the ORNL Graphite Reactor Shield	16
7	Gamma-Ray Dose Rate Along Hole in ORNL Graphite Reactor Shield as a Function of the Distance from the Reactor-Shield Interface	19
8	Fast-Neutron Dose Rate Along Hole in ORNL Graphite Reactor Shield as a Function of the Distance from the Reactor-Shield Interface	24
9	Response of Fast-Neutron Dosimeter to Mixed Radiation	28
10	Thermal-Neutron Flux in 4-5/8-in.-dia and 1-in.-dia Holes in the ORNL Graphite Reactor Shield	30
11	Specific Thermal-Neutron Activity of Indium Foils as a Function of the Foil Thickness	34

INTERNAL DISTRIBUTION

- | | | | |
|--------|---|----------|---|
| 1. | C. E. Center | 76. | J. A. Harvey |
| 2. | Biology Library | 77. | A. Simon |
| 3. | Health Physics Library | 78. | F. C. Maienschein |
| 4-5. | Central Research Library | 79. | C. E. Clifford |
| 6. | Reactor Experimental
Engineering Library | 80. | A. D. Callihan |
| 7-34. | Laboratory Records Department | 81. | R. R. Coveyou |
| 35. | Laboratory Records, ORNL R.C. | 82. | W. Zobel |
| 36. | A. M. Weinberg | 83. | F. L. Keller |
| 37. | L. B. Emiet (K-25) | 84. | C. D. Zerby |
| 38. | J. P. Murray (Y-12) | 85. | D. K. Trubey |
| 39. | J. A. Swartout | 86. | S. K. Penny |
| 40. | E. H. Taylor | 87. | R. W. Peelle |
| 41. | E. D. Shipley | 88. | H. M. Glen |
| 42. | A. H. Snell | 89. | L. B. Holland |
| 43-52. | E. P. Blizard | 90. | L. Jung |
| 53. | M. L. Nelson | 91. | E. G. Silver |
| 54. | W. H. Jordan | 92-93. | A. B. Reynolds |
| 55. | G. E. Boyd | 94. | C. D. Cagle |
| 56. | R. A. Charpie | 95. | G. W. Keilholtz |
| 57. | S. C. Lind | 96. | G. T. Chapman |
| 58. | F. L. Culler | 97. | G. deSaussure |
| 59. | A. Hollaender | 98. | V. R. Cain |
| 60. | J. H. Frye, Jr. | 99. | F. J. Muckenthaler |
| 61. | M. T. Kelley | 100. | R. B. Murray |
| 62. | J. L. Fowler | 101. | J. M. Miller |
| 63. | R. S. Livingston | 102. | H. Bertini |
| 64. | K. Z. Morgan | 103-108. | T. V. Blosser |
| 65. | T. A. Lincoln | 109. | K. M. Henry |
| 66. | A. S. Householder | 110. | H. Moran |
| 67. | C. P. Keim | 111. | S. Terasawa |
| 68. | C. S. Harrill | 112. | C. A. Preskitt |
| 69. | C. E. Winters | 113. | F. L. Friedman (consultant) |
| 70. | D. S. Billington | 114. | H. Goldstein (consultant) |
| 71. | H. E. Seagren | 115. | H. Hurwitz, Jr. (consultant) |
| 72. | D. Phillips | 116. | L. W. Nordheim (consultant) |
| 73. | A. J. Miller | 117. | R. R. Wilson (consultant) |
| 74. | M. J. Skinner | 118. | ORNL - Y-12 Technical
Library, Document
Reference Section |
| 75. | R. R. Dickison | | |

EXTERNAL DISTRIBUTION

119. R. K. Osborn, Department of Nuclear Engineering, University of Michigan, Ann Arbor, Michigan
120. Harold S. Davis, General Electric Co., Bldg. 762, Richland, Washington
121. Harold L. Hull, E. I du Pont de Nemours, du Pont Bldg., Wilmington, Delaware
122. R. Aronson, Technical Research Group, New York, N. Y.
123. F. A. Aschenbrenner, General Electric Co., Cincinnati, Ohio
124. H. E. Hungerford, Atomic Power Development Association, Inc., 1911 First St., Detroit 26, Michigan
125. J. Van Hoomissen, General Electric Co., Idaho
126. F. N. Watson, Lockheed, Marietta, Ga.
127. M. F. Valerino, General Nuclear Engineering Corp., P. O. Box 245, Dunedin, Fla.
128. J. B. Dee, Pratt and Whitney Aircraft, CANEL Division, East Hartford, Conn.
129. G. J. Rausa, The Martin Company, Baltimore, Maryland
130. R. D. Schamberger, Brookhaven National Laboratory
131. Harold H. Rossi, Department of Radiology, Columbia University, 630 West 168th St., New York 38, N. Y.
132. Henry E. Stone, Knolls Atomic Power Laboratory, Bulter Bldg., C-2, P. O. Box 1072, Schenectady, N. Y.
133. L. A. Bowman, WCLJX, Wright-Patterson AFB, Ohio
134. H. T. Gomberg, University of Michigan, Ann Arbor, Michigan
135. E. R. Taylor, Union Carbide Nuclear Company (ORGDP)
136. T. F. Wagner, Union Carbide Nuclear Company (ORGDP)
- 137-153. R. C. Reid, Chemical Engineering Department, Massachusetts Institute of Technology, Cambridge, Massachusetts
154. Division of Research and Development, AEC, ORO
- 155-758. Given distribution as shown in TID-4500 (13th ed., Rev., Feb. 15, 1958) under Physics and Mathematics Category (75 copies - OTS)